### Title: New observations confirm the progressive acidification in the Mozambique Channel

Nicolas Metzl<sup>1</sup>, Claire Lo Monaco<sup>1</sup>, Aline Tribollet<sup>1</sup>, Jean-François Ternon<sup>2</sup>, Frédéric Chevallier<sup>3</sup>, Marion Gehlen<sup>3</sup>

- 1 Laboratoire LOCEAN/IPSL, Sorbonne Université-CNRS-IRD-MNHN, Paris, 75005, France
- 2 MARBEC, Université de Montpellier, CNRS, Ifremer, IRD, 34203 Sète, France
- 3 Laboratoire LSCE/IPSL, CEA-CNRS-UVSQ, Université Paris-Saclay Gif-sur-Yvette, 91191, France

Correspondence to: Nicolas Metzl (nicolas.metzl@locean.ipsl.fr)

#### Abstract:

New observations obtained in 2021 and 2022 are presented and used to investigate the trend of the carbonate system (including pH<sub>T</sub> and aragonite saturation state,  $\Omega_{ar}$ ) in the southern sector of the Mozambique Channel. Using historical and new data in April-May we observed an acceleration of the acidification ranging from -0.012 decade<sup>-1</sup> in 1963-1995 to -0.027 (±0.003) decade<sup>-1</sup> in 1995-2022. Result from a neural network (FFNN) model for all seasons also suggests faster pH trend in recent decades, -0.011 decade<sup>-1</sup> over 1985-1995 and -0.018 decade<sup>-1</sup> over 1995-2022. In May 2022 we estimated  $\Omega_{ar}$  of 3.49, about 0.3 lower than observed in May 1963 ( $\Omega_{ar}$  = 3.86). The lowest  $\Omega_{ar}$  value of 3.23 was evaluated from the FFNN model in September 2023 that corresponds to the hypothetical critical threshold value (3.25) for coral reefs. In 2025 a marine heat wave was observed in this region (sea surface temperature up to 30°C) and data from a BGC-Argo float indicate that sea surface pH was the lowest in January 2025 (pH<sub>T</sub> = 7.95) whereas  $\Omega_{ar}$  was the lowest in Mach 2025 ( $\Omega_{ar}$  = 3.2). A projection of the C<sub>T</sub> concentrations based on observed anthropogenic CO<sub>2</sub> in subsurface water and future anthropogenic CO<sub>2</sub> emissions scenario, suggests that a risky level for corals ( $\Omega_{ar}$  < 3) could be reached as soon as year 2034.

**Keywords:** Ocean Acidification, Decadal Trend, Mozambique Channel

# 1 Introduction:

The ocean plays a major role in reducing the impact of climate change by absorbing more than 90% of the excess heat in the climate system (Cheng et al., 2025; Forster et al 2025) and about 25% of human released  $CO_2$  (Friedlingstein et al., 2025). The oceanic  $CO_2$  uptake also changes the chemistry of seawater reducing its buffering capacity (Revelle and Suess, 1957) and leading to a process known as ocean acidification (OA) with potential impacts on marine organisms and ecosystems (Fabry et al., 2008; Doney et al., 2009, 2020; Gattuso et al, 2015; Schönberg et al, 2017; Cornwall et al, 2021). Global ocean models or Earth System Models predict that, due to future anthropogenic  $CO_2$  emissions and global warming, the sea surface pH could decrease by 0.4 and aragonite saturation state ( $\Omega$ ar) could be as low as 3 in the tropics by 2100 (Hoegh-Guldberg et al, 2007; Kwiatkowski et al, 2020; Jiang et al, 2023; Findlay et al, 2025). However, current global ocean models cannot fully replicate observations and not yet simulating all processes that govern ocean acidification (e.g. seasonal cycles of  $C_T$  and  $A_T$ , accumulation of  $C_{ant}$ , etc...). Long-term observations of the carbonate system are needed to compare and validate model results (Tilbrook et al, 2019).

The first estimate of the decadal pH change based on  $CO_2$  fugacity (fCO<sub>2</sub>) observations in the global ocean (using SOCAT data, Bakker et al, 2014) suggests a decrease of pH ranging between -0.003 decade<sup>-1</sup> (±0.005) in the North Pacific and -0.024 decade<sup>-1</sup> (±0.005) in the Indian Ocean over 1981-2011 (Lauvset et al, 2015). Reconstruction methods also based on SOCAT observations evaluated a global ocean decrease of pH in surface waters of -0.0181 ( $\pm$  0.0001) decade<sup>-1</sup> (lida et al,

2021), -0.0166 ( $\pm$  0.0010) decade<sup>-1</sup> (Ma et al, 2023) and -0.017 ( $\pm$  0.004) decade<sup>-1</sup> (Chau et al, 2024). These studies also highlighted the regional differences of the pH and aragonite saturation state ( $\Omega$ ar) trends. This calls for dedicated studies at regional scale in order to better interpret the inter-annual to multi-decadal changes of the oceanic carbonate system as the trends and associated uncertainties depend on the data available. Compared to other basins, observations are sparse in the Indian Ocean (Lauvset et al, 2015; Bakker et al, 2016, 2024). However, thanks to a new cruise conducted in 2019, it has been shown that the Mozambique Channel experienced an acceleration with respect to  $\frac{1}{1}$  ( $\frac{1}{1}$  40.005) over 1995–2019 (Lo Monaco et al, 2021). In a more recent analysis Chakraborty et al (2024) used several methods, including a high resolution model dedicated to the Indian Ocean and found an acceleration of the pH trend of -0.011 ( $\frac{1}{1}$ 0.00) decade<sup>-1</sup> in 1980–1989 to -0.019 ( $\frac{1}{1}$ 0.004) decade<sup>-1</sup> in 2010–2019. Both studies concluded that strengthening of acidification trend was mainly driven by ocean CO<sub>2</sub> uptake.

In this study, we present new data obtained in January 2021 and April-May 2022 in the Mozambique Channel and used the results of a FFNN model (Chau et al, 2024) extended to 2023 to explore the decadal trends of the carbonate system over 1963-2023. We also use these data to validate a projection of the acidification in the near future. To highlight  $CO_2$  source anomalies when the ocean was exceptionally warm, results from a BGC-Argo float in the Mozambique Channel in 2024-2025 are also presented.

### 2 Data selection and methods

#### 2.1 Data selection

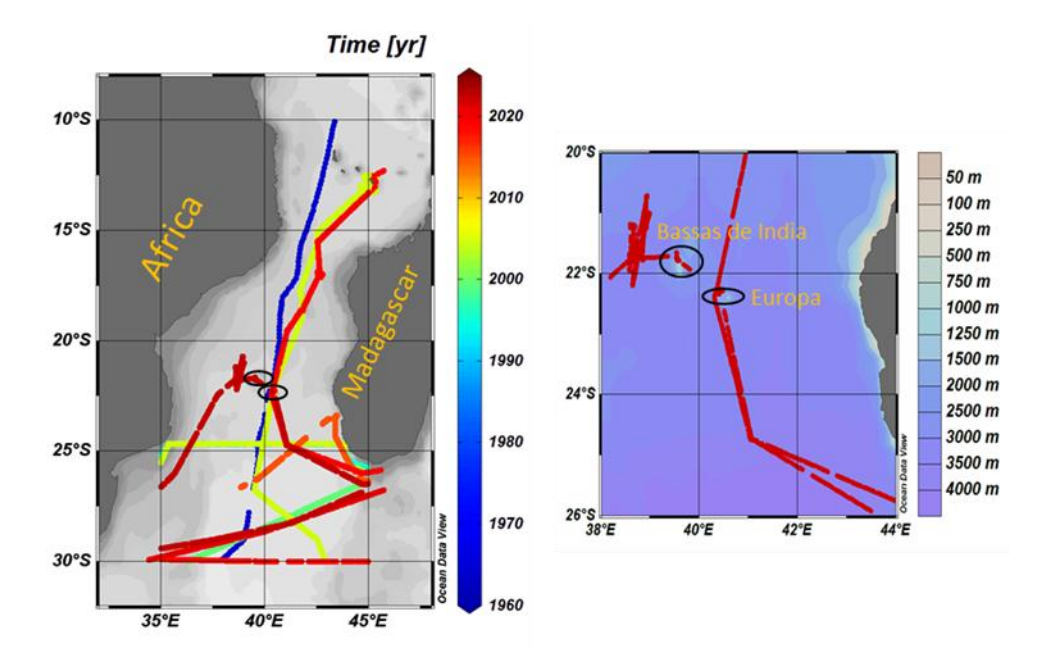
To explore the long-term change of the carbonate system in this region, we selected the fCO $_2$  SOCAT data, version v2024 (Bakker et al, 2016, 2024). With recent cruises conducted on-board the ship Marion-Dufresne in January 2021 (OISO-31) and April-May 2022 (RESILIENCE) this includes 10 cruises in the Mozambique Channel (Table 1 and Figure 1). Some of these cruises were previously described to analyze the distribution air-sea  $CO_2$  fluxes and pH changes in the Mozambique Basin and the African coastal zone (Metzl et al, 2025b). Here we focus on the data obtained in the southern Mozambique Channel. To complete the shipboard data after 2022 we also used data from a BGC-Argo float (WMO ID 7902123) that was launched onboard R/V Sonne in the Mozambique Channel in late 2024. During some cruises (2004, 2019 and 2021) continuous underway  $A_T$  and  $C_T$  measurements were also performed (data available in Metzl et al, 2025a). These  $A_T$  and  $C_T$  data are used to compare and validate results of the pH trends based on fCO $_2$  data.

Table 1: List of cruises in the Mozambique Channel from SOCAT-v2024 (Bakker et al, 2024).

91				
92	EXPOCODE	Month	Year	Reference or Principal Investigator
93				
94	31AR19630216	5	1963	Keeling and Waterman (1968)
95	316N19950611	6	1995	Key, R.
96	33RO19990211	2	1999	Wanninkhof, R.
97	49NZ20031209	12	2003	Murata, A.
98	35MF20040106(a)	1	2004	Metzl (2009)
99	06BE20140710	7	2014	Steinhoff, T., Koertzinger, A
100	33RO20180423	4	2018	Wanninkhof, R., Pierrot, D.
101	35MV20190405 (a)	4	2019	Lo Monaco et al. (2021)
102	35MV20210113 (a)	1	2021	Metzl et al. (2025b)
103	35MV20220420	4	2022	Metzl et al. (2025b)
104				

(a) For these cruises underway  $A_T$   $C_T$  data available at https://doi.org/10.17882/102337

Figure 1: Left: Tracks of cruises in the Mozambique Channel in the SOCAT data-base, version v2024 (Bakker et al., 2016; 2024). This includes recent OISO-31 and RESILIENCE cruises in 2021 and 2022. Color code is for Year. Black circles identified the coral reefs locations. Right: Tracks of cruises near the coral reefs area. Figures produced with ODV (Schlitzer, 2018).



## 2.2 Methods

The methods for surface underway  $fCO_2$  and  $A_T$   $C_T$  measurements were described in previous studies (e.g. Lo Monaco et al, 2021). For  $fCO_2$  measurements during OISO-11 (2004), CLIM-EPARSES (2019), OISO-31 (2021) and RESILIENCE (2022) cruises, sea-surface water was continuously equilibrated with a "thin film" type equilibrator thermostated with surface seawater (Poisson et al., 1993) and xCO2 in the dried gas was measured with a non-dispersive infrared analyzer (NDIR, Siemens Ultramat 6F). Standard gases for calibration (around 280 ppm, 350 ppm and 490 ppm) were

measured every 6 hours. The sea surface temperature (SST) and equilibrium temperature were measured using SBE21 and SBE38 probes (accuracy  $0.002^{\circ}$ C) respectively. During the RESILIENCE cruise the difference of SST and equilibrium temperature was on average +0.088 ±0.066 °C (n= 6416). For all cruises, the sea surface salinity (measured with SBE21) was regularly checked with discrete samples and has been corrected if some drift was observed. The fCO<sub>2</sub> in situ data were corrected for warming using corrections proposed by Copin-Montégut (1988, 1989). Note that when incorporated in the SOCAT data-base, the original fCO2 data are recomputed (Pfeil et al., 2013) using temperature correction from Takahashi et al. (1993). Given the very small difference between equilibrium temperature and sea surface temperature, the fCO<sub>2</sub> data from SOCAT used in this analysis (Bakker et al., 2024) are almost identical (within 1  $\mu$ atm) to the original fCO<sub>2</sub> values.

During 3 cruises, in January 2004 (OISO-11), April 2019 (CLIM-EPARSES) and January 2021 (OISO-31),  $A_T$  and  $C_T$  were measured continuously in surface water using a potentiometric titration method (Edmond, 1970) in a closed cell. For calibration, we used the Certified Referenced Materials provided by Pr. A. Dickson (SIO, University of California). Based on repeatability from duplicate analyses of continuous sea surface sampling at the same location (when the ship was stopped) we estimated the accuracy for both  $A_T$  and  $C_T$  better than 4 µmol.kg<sup>-1</sup> (Metzl et al, 2025a). The  $A_T$  and  $C_T$  data for these cruises are available at the Seanoe platform (https://doi.org/10.17882/102337). These data offered comparisons and validation for the calculations of the carbonate system properties using fCO<sub>2</sub> data and  $A_T$ /Salinity relationship.

## 2.3 Carbonate system calculation and A<sub>T</sub>/Salinity relationship

When two of the carbonate system properties are measured (here either fCO<sub>2</sub>,  $A_T$  or  $C_T$ ) they can be used to calculate other species and the saturation state of aragonite ( $\Omega_{ar}$ ). Here we used the CO2sys program (version CO2sys\_v2.5, Orr et al., 2018) with K1 and K2 dissociation constants from Lueker et al. (2000) and KSO4 constant from Dickson (1990). The total boron concentration is calculated according to Uppström (1974). When using fCO<sub>2</sub> data to derive pH<sub>T</sub> (pH<sub>T</sub> for Total Scale) or C<sub>T</sub>, one needs A<sub>T</sub> concentrations that can be derived from salinity (e.g. Millero et al, 1998). Here we used the A<sub>T</sub>/Salinity relationship adapted to the Mozambique Channel (Lo Monaco et al, 2021).

 $A_T$  (µmol.kg-1) = 73.841 (± 1.15) \* SSS – 291.02 (± 40.4) (n= 548,  $r^2$  = 0.88) (Eq. 1)

## 2.4. CMEMS-LSCE-FFNN model

The fCO $_2$  data are not available each year and only for few seasons (Table 1). To complete the observations we used the results from an ensemble of feed-forward neural network model (CMEMS-LSCE-FFNN or FFNN for simplicity here, Chau et al., 2024). Based on the SOCAT gridded datasets this model composes surface ocean carbonate system fields at 0.25 x 0.25 square degree resolution and monthly scale. The reconstructed fCO $_2$  is used to derive monthly surface C $_T$ , pH $_T$  and aragonite and calcite saturation states, as well as air-sea CO $_2$  fluxes. A full description of the model is presented in Chau et al (2024) and the datasets including uncertainties are available under the DOI https://doi.org/10.48670/moi-00047.

#### 3 Results and discussion

### 3.1 A Repeated line in 2019 and 2022

In April 2019 and 2022 underway measurements were conducted for  $fCO_2$ . The measurements of  $A_T$  and  $C_T$  were also performed in 2019. The tracks of the cruises enabled to select the data obtained along the same track and for the same season in the southern Channel in order to compare the observations three years apart (Figure 2). Given the variability observed around Europa

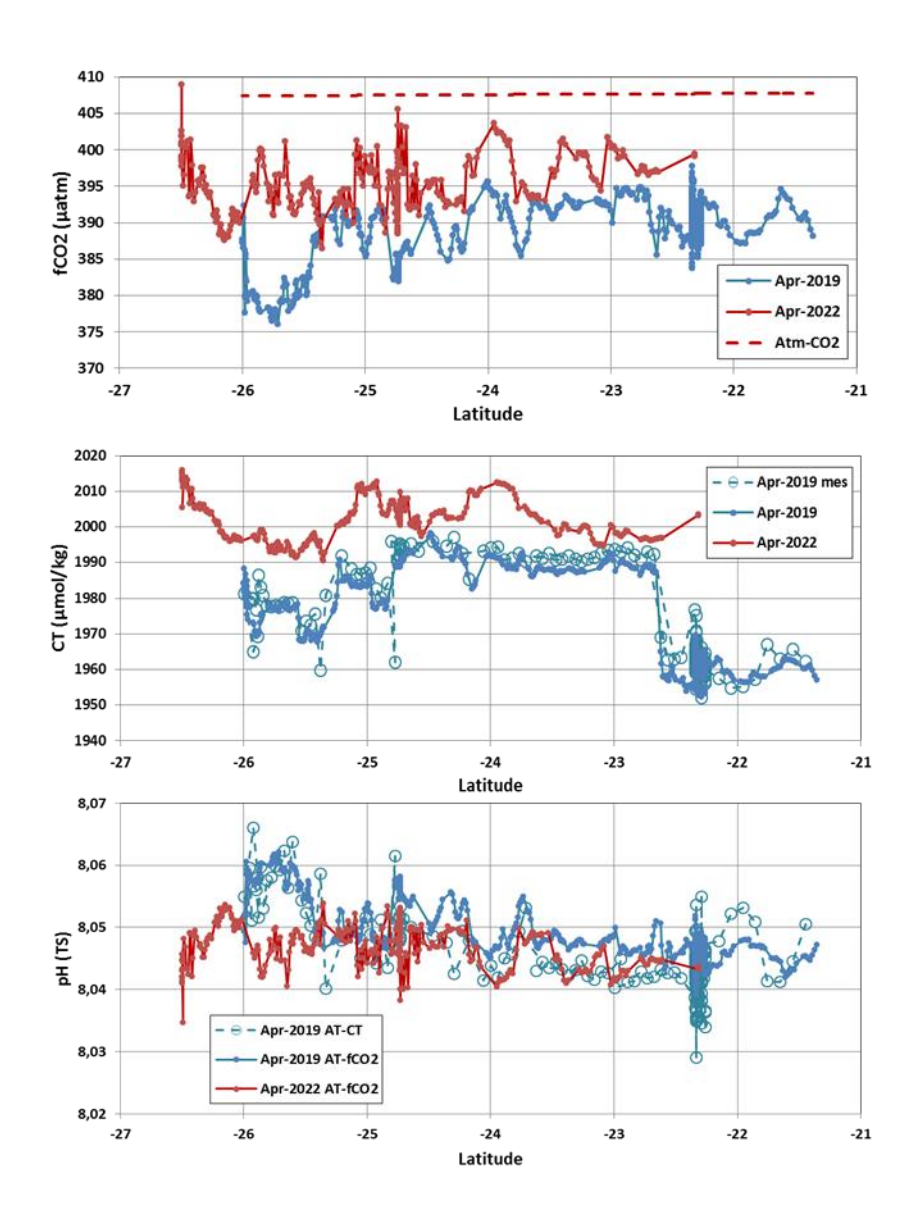
Island and the front identified at 22.5°S in April 2019 (Figure 2) the data were averaged in the band 23°-26°S. The mean values over the same latitudinal band (23-26°S) show significant differences between 2019 and 2022 (Table 2). In 2022 the ocean was slightly colder and saltier. Consequently,  $A_T$  concentrations were also higher in 2022 but the salinity normalized  $A_T$  (N- $A_T$  normalized at salinity 35) were the same with a difference of +1.1  $\mu$ mol.kg<sup>-1</sup>. As expected, due to the  $CO_2$  uptake, the oceanic  $fCO_2$  and  $C_T$  concentrations were higher in 2022 and  $pH_T$  was lower. The increase of oceanic  $fCO_2$  over 3 years (+7.9  $\mu$ atm) was almost the same as in the atmosphere (+7.0  $\mu$ atm). At constant  $A_T$ , salinity and temperature, the observed  $fCO_2$  change would translate in an increase of +4.4  $\mu$ mol.kg<sup>-1</sup> for  $C_T$  when we observed an increase of +18  $\mu$ mol.kg<sup>-1</sup> (Table 2). We interpret this difference as being due to the regional circulation. In April 2019 southward currents would import low  $C_T$  and  $A_T$  whereas in April 2022 northward currents would transport colder and saltier waters with higher  $C_T$  and  $A_T$ . This reversed circulation is confirmed with the ADCP data recorded during the cruises as well as from the geostrophic currents (Metzl et al, 2022; Ternon et al, 2023).

For pH<sub>T</sub>, the decrease of -0.005 over three years, i.e. -0.0017 yr<sup>-1</sup>, is surprisingly close to what is generally observed at global scale and over several decades (-0.0017  $\pm 0.0004$ .yr<sup>-1</sup>, Chau et al, 2024). Finally, we note that the difference between 2019 and 2022 measurements is much higher than that obtained when comparing measured and calculated A<sub>T</sub> C<sub>T</sub> values (Table 2). This confirms the use of fCO<sub>2</sub> data and adapted A<sub>T</sub>/S relationship to derive the carbonate system properties in this region (Lo Monaco et al, 2021; Metzl et al, 2025b), and to explore the seasonal cycles and long-term trends described in the next sections.

Table 2: Mean values of underway sea surface observations and their difference obtained along the same track in 2019 and 2022 in the region 23-26°S (see Figure 2). Nb is the number of data. Standard-deviations are in bracket. For 2019 (CLIM-EPARSES cruise), the results from underway  $A_T-C_T$  measurements are listed allowing calculation of  $fCO_2$  and pH based on the  $A_T-C_T$  pairs which permit comparisons with those derived from  $fCO_2$  measurements.

Cruise Period	Nb	SST °C	SSS -	A <sub>τ</sub> μmol.k <sub>i</sub>	C <sub>T</sub>	fCO <sub>2</sub> μatm	pH <sub>T</sub> TS	Atm. xCO2 ppm
RESILIENCE fCO <sub>2</sub>	282	26.765	35.423	2324.6	2002.0	394.8	8.047	414.7
April 2022		(0.608)	(0.048)	(3.6)	(5.0)	(3.4)	(0.003)	
CLIM-EPARSES fCO <sub>2</sub>	294	27.497	35.288	2314.7	1984.0	386.9	8.053	407.5
April 2019		(0.341)	(0.084)	(6.2)	(7.5)	(4.9)	(0.004)	
CLIM-EPARSES A <sub>T</sub> -C <sub>T</sub>	70	27.401	35.272	2314.2	1986.1	389.7	8.050	
April 2019		(0.390)	(0.099)	(6.7)	(8.8)	(7.4)	(0.006)	
Difference Method 203	19	+0.096	+0.016	+0.5	-2.1	-2.9	+0.002	
Difference 2022-2019		-0.732	+0.135	+10.0	+18.0	+7.9	-0.005	+7.2

Figure 2: Distribution of measured  $fCO_2$  ( $\mu$ atm), calculated  $C_T$  ( $\mu$ mol/kg) and calculated  $pH_T$  (TS) along a repeated track in April 2019 (blue) and April 2022 (red) in the southern Mozambique Channel. The dashed red line is for atmospheric  $fCO_2$  in 2022. The underway  $C_T$  measurements in 2019 are also shown (open circles) as well as  $pH_T$  calculated using measured  $A_T$  and  $C_T$ . Average values for the latitudinal band 23-26°S are presented in Table 2.



### 3.2 Seasonal variations

In the Mozambique Channel, where SST presents large seasonal variations (up to 4°C), fCO<sub>2</sub> is mainly controlled by temperature like in the Indian subtropics (e.g. Metzl et al 1998; Takahashi et al, 2002; Bates et al, 2006). In this region, observations are not available for all seasons (Table 1) but the seasonal range derived from the climatology (Fay et al, 2024) or the FFNN model (Chau et al, 2024) is coherent compared to the data (Figure 3, Figure S1). The observations and the models indicate that between January and July fCO<sub>2</sub> decreases by about 50  $\mu$ atm while pH<sub>T</sub> increases (0.03 to 0.04 units). This is a large signal compared to the expected decadal change (about +20  $\mu$ atm.decade<sup>-1</sup> for fCO<sub>2</sub> and -0.017.decade<sup>-1</sup> for pH<sub>T</sub>); therefore, to derive and interpret the trends, data have to be selected for the same season. As opposed to fCO<sub>2</sub>, C<sub>T</sub> presents lower concentrations in February-April and higher ones in July-August (Figure 4). When the mixed-layer depth (MLD) is shallow in December-March the decrease of C<sub>T</sub> is probably linked to biological activity but this is not clearly quantified (Lo

Monaco et al, 2021). The progressive  $C_T$  increase of about +30  $\mu$ mol.kg<sup>-1</sup> from March to August is likely driven by vertical mixing when MLD is deeper in austral winter (Figure 4).

This seasonality was well observed from repeated measurements at stations located along 25°S in June 1995 and December 2003 (Figure S2). In June 1995 when the MLD reached 80 m,  $C_T$  concentrations were homogeneous within the MLD layer. The same was true for the anthropogenic  $CO_2$  concentrations ( $C_{ant}$ ) here evaluated using the TrOCA method (Touratier et al. 2007). On the opposite, in December 2003, when the MLD was shallower,  $C_T$  presented a sharp increase within the subsurface layer whereas  $C_{ant}$  concentrations were unrealistic in surface seawaters. Although from 1995 to 2003 the  $C_T$  concentrations would increase by around +7  $\mu$ mol/kg due to the anthropogenic  $CO_2$  uptake in that region (Murata et al, 2020; Metzl et al, 2025b), N- $C_T$  (normalized  $C_T$  at salinity 35) in June 1995 were almost the same as in December 2003 coherent with the seasonal cycle derived from the climatology (Figure 4).

The seasonal variations of  $fCO_2$  and  $pH_T$  in the Mozambique Channel appear thus linked to both temperature and mixing process with competition between the two drivers (Figure S3). In addition to the rising atmospheric  $CO_2$ , these two processes probably also drive inter-annual, decadal and long-term change of  $fCO_2$  and  $pH_T$  in the region as the Indian Ocean experienced a pronounced warming (Cheng et al., 2025). Specifically, in the southern Mozambique Channel the SST has increased by  $+0.11 \pm 0.009$  °C per decade since the 1960s (Figure S4), a signal that should be taken into account when interpreting the decadal trends of carbonate properties and  $CO_2$  fluxes. In January 2025 the SST anomaly reached +1.6°C at 25°S in the Channel.

Figure 3: Seasonal cycle of (a)  $fCO_2$  ( $\mu$ atm) and (b)  $pH_T$  in the southern Mozambique Channel (24-30°S). Average observations are presented for each cruise (colored circles). The full seasonal cycles are shown for the monthly climatology (reference year 2010, Fay et al, 2024) and for the FFNN model for years 2010 and 2022 with respective error bars.

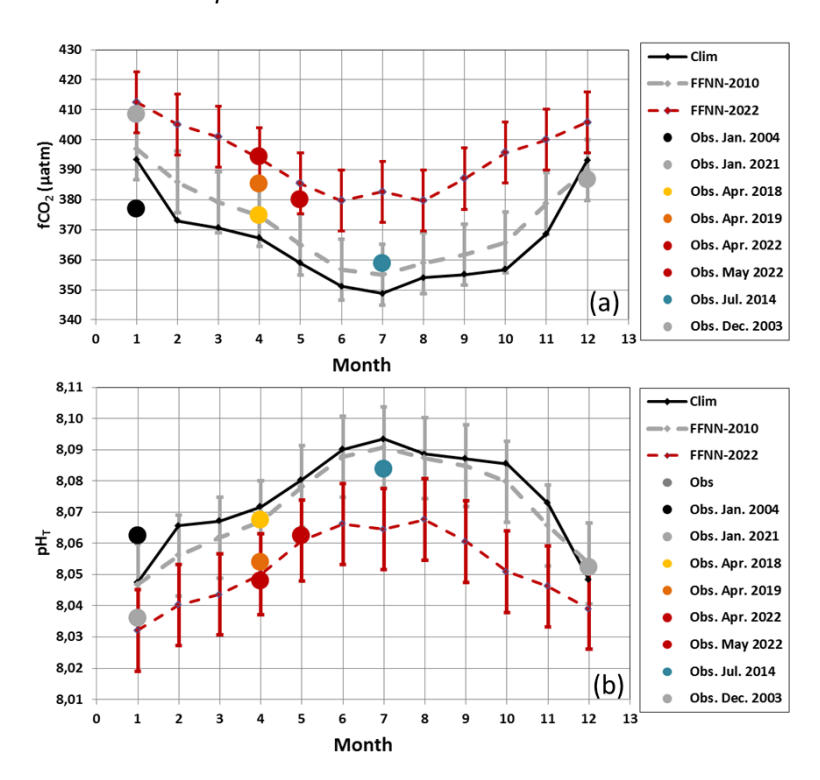
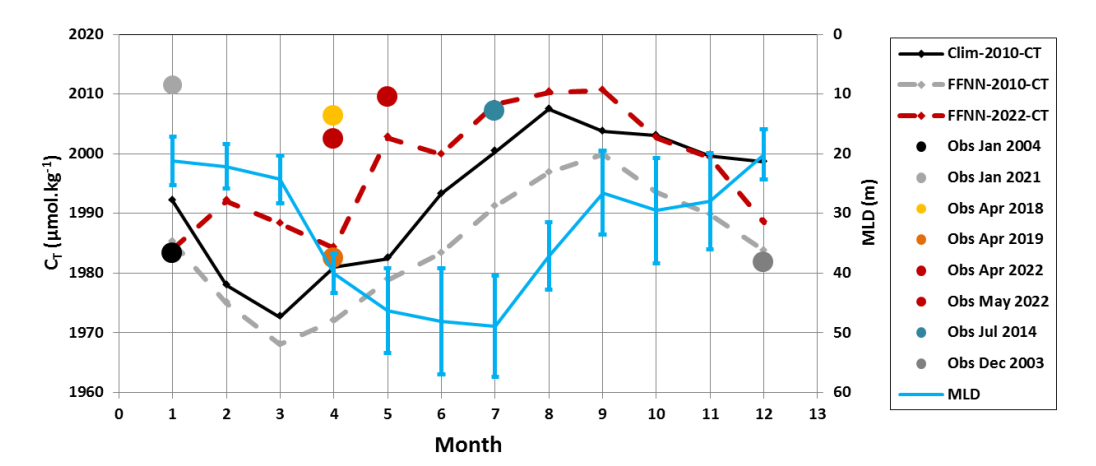


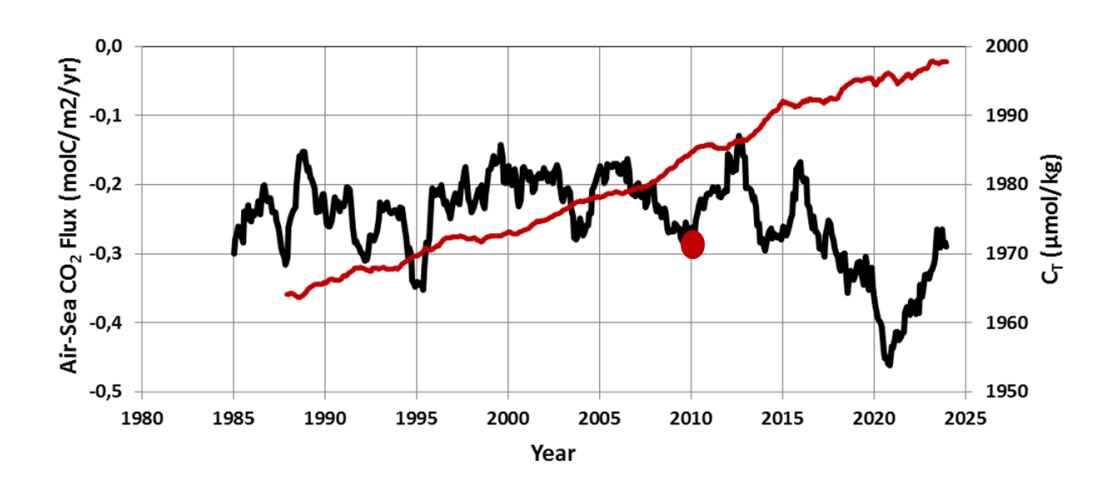
Figure 4: Seasonal cycle of  $C_T$  (µmol.kg<sup>-1</sup>) in the southern Mozambique Channel (24-30°S). Average observations are presented for each cruise (colored circles). The full seasonal cycles are shown based on the monthly climatology for a reference year 2010 (Fay et al, 2024) and the FFNN-LSCE model for year 2010 (Chau et al, 2024). The mixed-layer depth (MLD in m, blue line) is averaged in this region (from multi-year reprocessed monthly data, ARMOR3D L4, https://doi.org/10.48670/moi-00052, last access 20/4/2025).



### 3.3 Trends in the Southern Mozambique Channel (1963-2023)

In this region, the ocean is a permanent  $CO_2$  sink leading to a gradual increase of  $C_T$  concentrations and decrease of  $pH_T$ . The air-sea  $CO_2$  flux derived from the FFNN model is on average -0.249 (±0.063) molC.m<sup>-2</sup>.yr<sup>-1</sup> (Figure 5) in the range of the climatology (-0.3 molC.m<sup>-2</sup>.yr<sup>-1</sup>, Fay et al, 2024). The FFNN model also suggests that the sink reinforced over 2016-2021 with a perceptible faster increase of  $C_T$  (Figure S5).

Figure 5: Time-series of air-sea  $CO_2$  flux (black, negative for ocean sink) and  $C_T$  concentration (red) averaged in the southern Mozambique Channel (24-30°S) based on the FFNN-LSCE model over 1985-2023. For  $C_T$ , the result is presented with a 36-month running mean. Also shown is the climatological value of the flux for year 2010 in this region (red circle, Fay et al, 2024).



#### 3.3.1 Decadal trend from fCO<sub>2</sub> and A<sub>T</sub> C<sub>T</sub> data: January 2004 and 2021

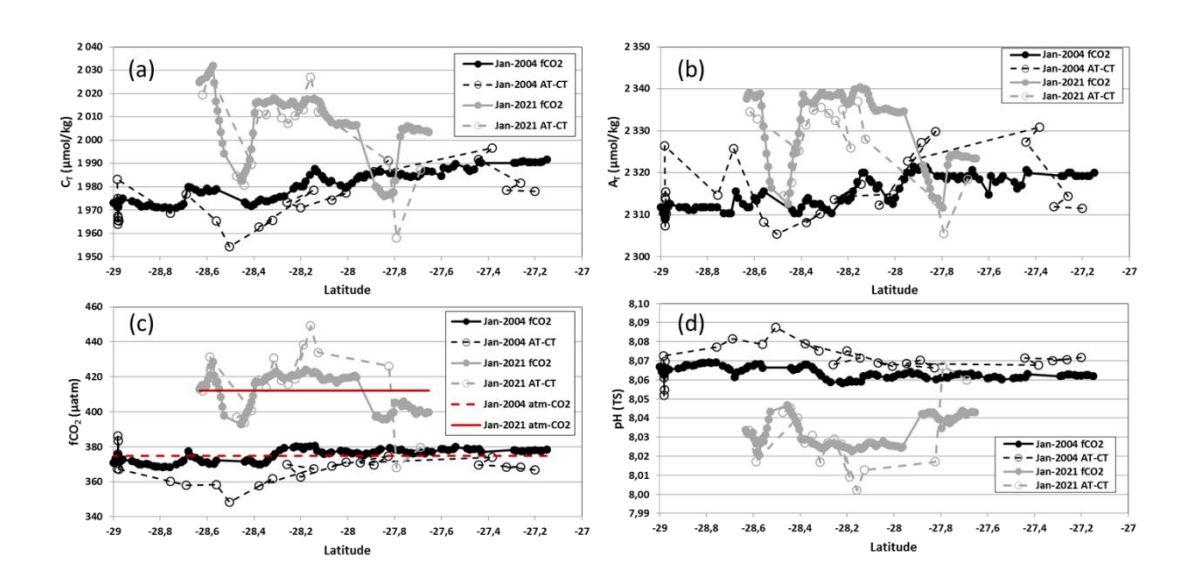
We started the analysis of the decadal change by comparing observations obtained in January 2004 and 2021 when data were available for both underway fCO<sub>2</sub>,  $A_T$  and  $C_T$  measurements. The comparison is focused along the tracks occupied in the same region (27-29°S/40-43°E, Figure 6,

Table 3). For both cruises the differences between measurements and calculations are in the range of the errors in the CO2sys calculations (errors on measurements and constants K<sub>1</sub>, K<sub>2</sub>, Orr et al., 2018). For example, in January 2004 the pH<sub>T</sub> calculated with  $A_T$  and  $C_T$  measurements was 8.069 against 8.064 when using the fCO<sub>2</sub> data and the A<sub>T</sub>/S relationship. In 2021 the pH<sub>T</sub> were respectively 8.030 and 8.032 (Table 3). For C<sub>T</sub> the difference between calculated and measured C<sub>T</sub> was only 4.4 μmol.kg  $^{1}$  in 2004 and -1.9  $\mu$ mol.kg $^{-1}$  in 2021 when the observed increase over 17 years is around 28  $\mu$ mol.kg $^{-1}$ <sup>1</sup>. We noticed that in 2021, the properties present a high variability along the track linked to the presence of eddies. The  $C_T$  and  $A_T$  concentrations could vary by about 20 to 40  $\mu$ mol.kg<sup>-1</sup> at mesoscale but this has a small impact on calculated fCO<sub>2</sub> and pH<sub>T</sub>, and when properties are averaged along the track (Table 3). For both periods the ocean fCO2 was close to atmospheric CO2, i.e. near equilibrium (fCO<sub>2</sub> ocean-fCO<sub>2</sub> atm =  $\Delta$ fCO<sub>2</sub> = -0.04 ±3.11 µatm in 2004 and 0.37 ±10.04 µatm in 2021). Although there were some differences of pH<sub>T</sub> calculated from the two data-sets (underway fCO<sub>2</sub> or A<sub>T</sub>  $C_T$  data), the estimated  $pH_T$  change of -0.032 or -0.040 over 17 years was large compared to the uncertainty of the CO2sys calculation. This would correspond to a pH<sub>T</sub> trend varying between -0.0019 and -0.0023.yr<sup>-1</sup>. This comparison of observations in January 2004 and 2021 supports the use of the selected  $A_T/S$  relationship for pH calculations based on all  $fCO_2$  data available over 1963–2023 in order to explore the long-term trend described in the next section.

 Table 3: Mean values of underway sea surface observations and their difference obtained in the same region (27-29°S/40-43°E) in January 2004 and 2021. Nb is the number of data. Standard-deviations are in bracket. The results are presented for both methods (underway fCO<sub>2</sub> or  $A_T$ - $C_T$  measurements) and fCO<sub>2</sub>, pH<sub>T</sub> calculated with  $A_T$ - $C_T$  pairs compared with those derived from fCO<sub>2</sub> measurements. The last lines are the difference for 2021 minus 2004 and errors associated to the measurements or calculations (\*).

— Cr	uise Method	Nb	SST	SSS	Α <sub>τ</sub>		fCO <sub>2</sub>	 рН <sub>Т</sub>	Atm. xCO <sub>2</sub>
	eriod		°C	-	μmol.k		μatm	TS	ppm
01	SO-11 fCO <sub>2</sub>	140	27.293	35.282	2314.2	1978.5	374.7	8.064	374.8
	nuary 2004		(0.331)	(0.050)	(3.7)	(6.7)	(3.2)	(0.002)	
O	SO-11 A <sub>T</sub> -C <sub>T</sub>	30	27.516	35.248	2315.4	1974.1	368.7	8.069	
Ja	nuary 2004		(0.609)	(0.042)	(7.2)	(9.8)	(7.6)	(0.007)	
Ol	SO-31 fCO <sub>2</sub>	102	27.825	35.508	2330.9	2006.8	412.5	8.032	412.2
Ja	nuary 2021		(0.793)	(0.118)	(8.7)	(14.1)	(10.0)	(0.008)	
Ol	SO-31 A <sub>T</sub> -C <sub>T</sub>	17	27.916	35.515	2326.9	2003.5	414.4	8.030	
Ja	nuary 2021		(0.678)	(0.139)	(9.6)	(18.7)	(21.2)	(0.017)	
Di	fference 2021-2004								
Uı	nderway fCO <sub>2</sub>		0.532	0.225	16.7	28.3	37.8	-0.032	37.4
Uı	nderway A <sub>T</sub> -C <sub>T</sub>		0.400	0.267	11.5	29.4	45.7	-0.040	
Er	ror using fCO <sub>2</sub>		0.01	0.01	4	7.3 *	2	0.014*	
Er	ror using A <sub>T</sub> -C <sub>T</sub>		0.01	0.01	4	4	13.9*	0.007*	

Figure 6: Distribution of measured or calculated  $C_T$  (a,  $\mu$ mol  $kg^{-1}$ ),  $A_T$  (b,  $\mu$ mol  $kg^{-1}$ ),  $fCO_2$  (c,  $\mu$ atm) and  $pH_T$  (d) along the same track in January 2004 (black symbols) and January 2021 (grey symbols). Values derived from  $fCO_2$  measurements are in filled symbols/lines, those from the  $A_T$   $C_T$  measurements in open symbols/dashed lines. In (c) the red lines represent the atmospheric  $CO_2$  in 2004 and 2021. Average values and their differences are presented in Table 3.



## 3.3.2 Multi-decadal trends from fCO<sub>2</sub> data (1963-2023)

 For long-term trends, we used fCO<sub>2</sub> observations and observations-based reconstructions averaged in the region 24-30°S (Table 4). As the observations are not available for all seasons, we selected the period April-May to calculate the trends from the data (same season for the first and the last cruises in 1963 and 2022) whereas the FFNN model offers information for all seasons. Back in the 1960s, the observations in 1963 indicate that the ocean was a CO<sub>2</sub> sink in May (Figure 7a), the value of  $\Delta$ fCO<sub>2</sub> = -32.2  $\mu$ atm being almost the same as observed in May 2022 ( $\Delta$ fCO<sub>2</sub> = -32.5  $\mu$ am). This suggests a strong link between ocean and atmospheric fCO<sub>2</sub> (Figure S6).

For the first observational period, the changes between 1963 and 1995 indicated a pH<sub>T</sub> decrease of -0.040. Over 32 years this pH<sub>T</sub> change was driven by the C<sub>T</sub> increase (effect on pH<sub>T</sub>= -0.045), the A<sub>T</sub> increase (effect on pH<sub>T</sub>= +0.012) and the warming of 0.95°C (effect on pH<sub>T</sub>= -0.015). Between 1995 and 2022 the observed decrease accelerated to -0.0027 (±0.0003) yr<sup>-1</sup> (Table 4). In contrast, the neural network suggested smaller pH<sub>T</sub> trends. However, as in the observations, the annual pH<sub>T</sub> change from the model was faster in recent decades (-0.0018 yr<sup>-1</sup> over 1995-2022 against -0.0011 yr<sup>-1</sup> over 1985-1995, Table 4). The model also suggested different trends depending on the season. The pH<sub>T</sub> trend appeared indeed faster in July (when the ocean CO<sub>2</sub> sink is stronger) than in January or April (Table 4).

The new data in 2021 and 2022 and the FFNN model extended to 2023 confirmed a previous analysis in the Mozambique Channel (Lo Monaco et al, 2021) with a pH $_{\rm T}$  trend of -0.0023 yr $^{-1}$  (±0.00048) over 1995–2019. Our new results in the southern Mozambique Channel are also in the range of the pH $_{\rm T}$  trends previously evaluated at basin scale in the Indian Ocean, -0.0027 yr $^{-1}$  (±0.0005) over 1991-2011 (Lauvset et al, 2015). High resolution ocean models applied to the northern Indian Ocean also suggest an acceleration of the acidification, with pH $_{\rm T}$  trend reaching -0.0019 yr $^{-1}$  (±0.0004) in 2010–2019 (Chakraborty et al, 2024), somehow lower than our estimate based on observations at regional scale in the Mozambique Channel (-0.0027 yr $^{-1}$  ±0.0003 in 1995-2022, Table 4).

Table 4: Trends of properties in the southern Mozambique Channel derived from observations and the FFNN model. For observations, the trends are evaluated for April-May season only (based on few data-points identified as red circles in Figure 7). For FFNN, trends are estimated for all seasons or only for January, April, May and July. Standard-deviations are in bracket.

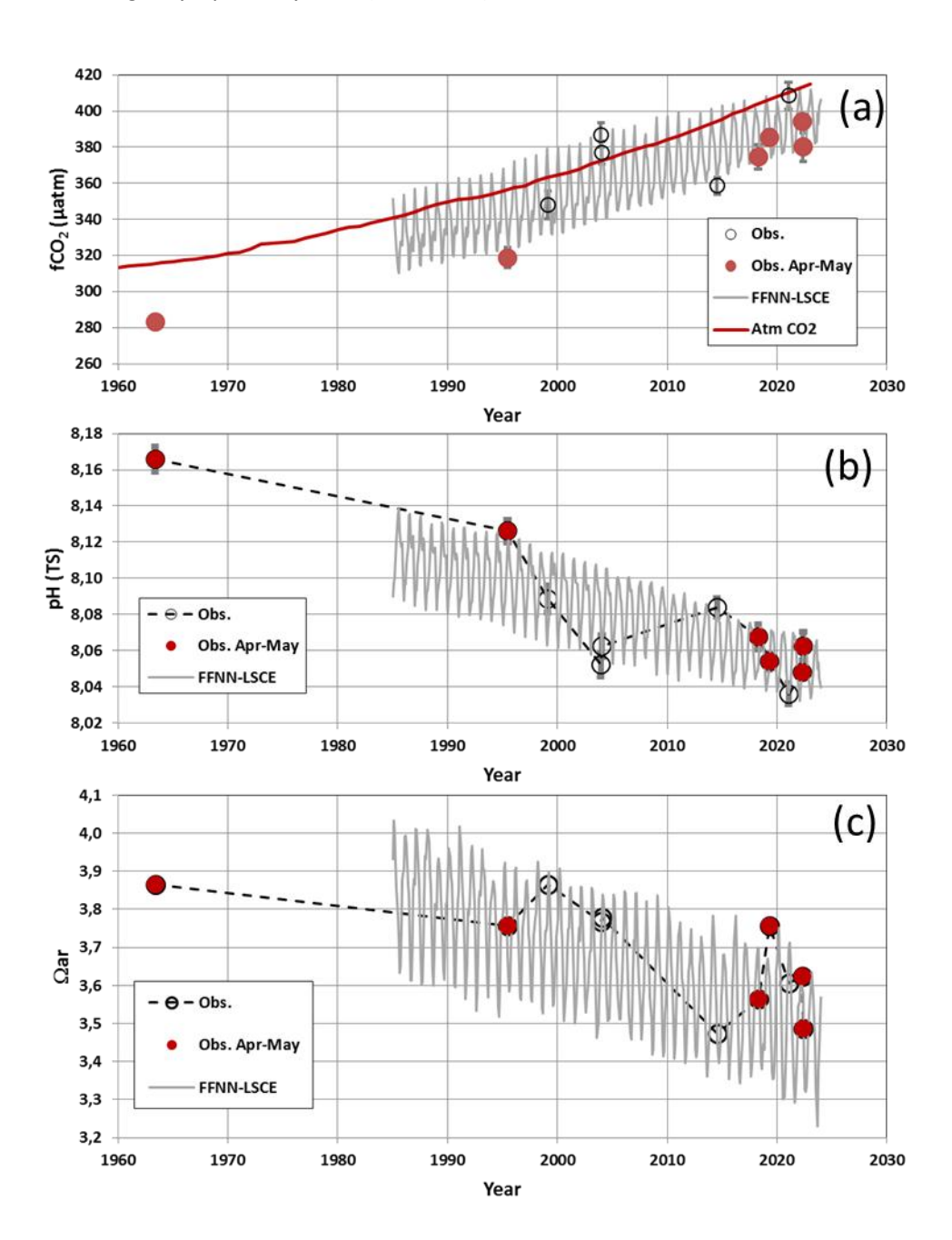
Method	Period	fCO <sub>2</sub> μatm.yr <sup>-1</sup>	C <sub>τ</sub> μmol.k	A <sub>T</sub> g.yr <sup>-1</sup>	pH <sub>T</sub> TS.yr <sup>-1</sup>
Obs April-May	1963-1995	1.11	0.91	0.52	-0.0012
Obs April-May	1963-2022	1.84 (0.21)	0.69 (0.20)	0.08 (0.13)	-0.0020 (0.0002
Obs April-May	1995-2022	2.57 (0.30)	0.49 (0.52)	-0.34 (0.22)	-0.002 (0.0003
FFNN annual	1985-2023	1.76 (0.05)	0.99 (0.04)	0.02 (0.02)	-0.001 (0.000
FFNN annual	1985-1995	1.15 (0.34)	1.03 (0.29)	0.00 (0.08)	-0.001 (0.0004
FFNN annual	1995-2022	1.84 (0.09)	1.10 (0.07)	0.06 (0.03)	-0.0018 (0.000)
FFNN January	1985-2023	1.61 (0.03)	0.75 (0.07)	0.00 (0.05)	-0.0015 (0.0000
FFNN April	1985-2023	1.74 (0.03)	1.01 (0.07)	0.03 (0.07)	-0.001 (0.0000
FFNN May	1985-2023	1.71 (0.03)	1.07 (0.05)	0.07 (0.05)	-0.001 (0.0000
FFNN July	1985-2023	1.97 (0.04)	1.17 (0.05)	0.04 (0.02)	-0.0020

The aragonite saturation state  $(\Omega_{ar})$  was lower during austral summer (July-September). In May 1963, we estimated an aragonite saturation state of 3.86 (Figure 7c). It dropped to 3.49 in May 2022, a value close to that observed in July 2014 (3.47). The lowest  $\Omega_{ar}$  value of 3.23 was identified in September 2023 from the FFNN model. At that period,  $\Omega_{ar}$  was lower than 3.3 in the south of 20°S in the Mozambique Channel (Figure S7). This is close to the hypothetical critical threshold of  $\Omega_{ar}$  = 3.25, i.e. a risky level for coral reefs in the ocean claimed by Hoegh-Guldberg et al., (2007). Note that there are reefs know to thrive at  $\Omega_{ar}$  <3.0 like at volcanic  $CO_2$  seeps in Papua New Guinea ( $\Omega_{ar}$  = 2.41, Strahl et al 2015; see also review by Camp et al. 2018) but that their species composition and coral cover are different than at ambient conditions (i.e.  $\Omega_{ar}$ >3.3 considering Hoegh-Gulberg et al 2007). However, Strahl et al (2015) showed that calcification rate seems to vary among coral species, suggesting take conclusions of Hoegh-Gulberg et al (2007) with caution. With an annual trend of -0.010.yr<sup>-1</sup> for  $\Omega_{ar}$  over 1985-2023, a value of 3.3 would be reached in 2060 in summer whereas it was already observed in 2020 in winter with possible consequences on reef species composition and functioning (Tribollet al 2009, 2019; Schönberg et al 2017; Camp et al. 2018; Eyre et al. 2018; Cornwall et al 2021).

Although there are differences depending on the season and the method (in-situ observations, extrapolation of sparse in-situ observations through a FFNN model) all results suggest

an acceleration of the acidification in the last few years (Table 4, Figure 7) and a decrease of  $\Omega_{ar}$  that are mainly driven by the  $C_T$  increase through continuous ocean  $CO_2$  uptake (Ma et al, 2023). Given the rapid change of atmospheric  $CO_2$  in the recent years (up to +3.77 ppm.yr<sup>-1</sup> in 2024, Lan et al, 2025) how the carbonate system will change in the near future in this region and will impact corals reefs that are abundant (from Europa to Mayotte in the Mozambique Chanel) and subject to global warming, marine heat waves (e.g. Mawren et al, 2022; Alaguarda et al. 2022), ocean acidification, higher frequency of tropical cyclones and anthropogenic pressures (overfishing for instance), remains an important question.

Figure 7: Time-series of fCO<sub>2</sub> (a),  $pH_T$  (b) and  $\Omega_{ar}$  (c) in the southern Mozambique Channel (24-30°S) based on averaged observations (circles) and the FFNN-LSCE model over 1985-2023. In (a) the red line represents the atmospheric CO<sub>2</sub>. Available observations are shown for all seasons but the trends (Table 4) evaluated using only April-May data (red circles).



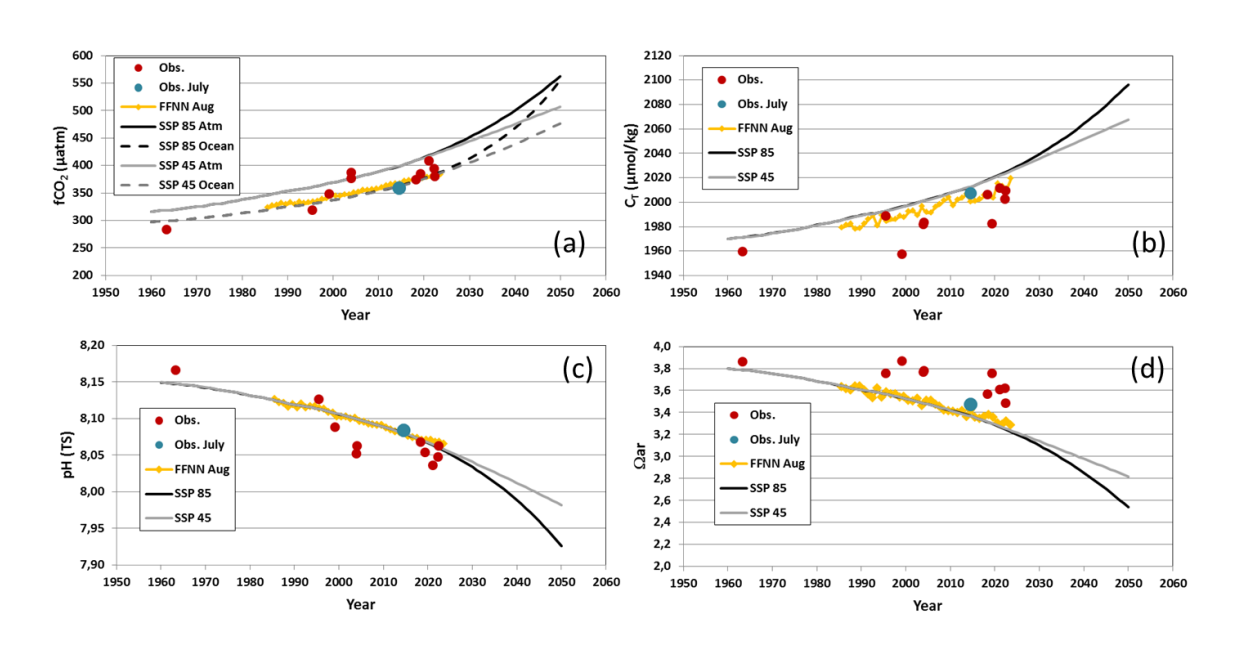
### 3.4 Projection in the near future

A recent analysis found that the  $C_{ant}$  concentrations in subsurface water in the Mozambique Basin were positively related to atmospheric  $CO_2$  with a slope of +0.512 ±0.050 µmol kg<sup>-1</sup> µatm<sup>-1</sup> (Metzl et al, 2025b, Figure S8). Here, we assume that this relationship is valid for the southern Mozambique Channel. To reconstruct the past and future change of the carbonate system properties we calculated the  $C_T$  concentration over 1960-2100 by correcting  $C_T$  for each year using the relationship between  $C_{ant}$  and atmospheric  $CO_2$ .

$$C_T(t) = C_T(t-1) + C_{ant}(t) - C_{ant}(t-1)$$
 (Eq. 2)

For future atmospheric  $CO_2$ , we used two SSP emissions scenarios (Shared Socioeconomic Pathways, Meinshausen et al., 2020), a "high" emission scenario SSP5-8.5 and a stabilization scenario SSP2-4.5 (Figure 8a). To explore the change of the aragonite saturation state, we applied this model (Eq. 2) for August when  $\Omega_{ar}$  is the lowest. Temperature and salinity were fixed from the climatology in August (SST =22.685 °C; SSS = 35.303) and fCO<sub>2</sub>, pH<sub>T</sub> and  $\Omega_{ar}$  were calculated each year with the C<sub>T</sub> A<sub>T</sub> pairs using version CO2sys\_v2.5 (Orr et al, 2018). The reconstructed C<sub>T</sub>, fCO<sub>2</sub>, pH<sub>T</sub> and  $\Omega_{ar}$  for August compared well with the observations (in July) and with the FFNN model in August (Figure 8; Table S1, Figure S9) indicating that the simulation captured the decadal evolution of the properties. For the future, differences between the two scenarios (SSP5-8.5 and SSP2-4.5) are pronounced after 2030 (Figure 8). For the high scenario the C<sub>T</sub> concentrations reaches 2060 µmol.kg<sup>-1</sup> in 2040 and pH<sub>T</sub> is as low as 8. In both scenarios, the carbonate ion concentrations dropped below 200 µmol.kg<sup>-1</sup> in 2028. As noted above, the aragonite saturation state based on observations was 3.47 in July 2014 (Figure 7c and blue symbol in Figure 8d) and the lowest  $\Omega_{ar}$  value of 3.23 occurred in August-September 2023 (from the FFNN model, Figure 7c and 8d). The same is estimated in the projection (Figure 7d), close to the critical threshold of  $\Omega_{ar}$  = 3.25 for tropical coral reefs.

Figure 8: Time-series of (a) atmospheric and oceanic  $fCO_2$ , (b)  $C_T$  concentrations, (c)  $pH_T$  and (d)  $\Omega_{ar}$  in the southern Mozambique Channel based on a reconstruction for August for two scenario (SSP85, black line, SSP45 grey lines). Averaged observations (all seasons, July in blue) and the FFNN-LSCE model over 1985-2023 in August (orange) are also shown.



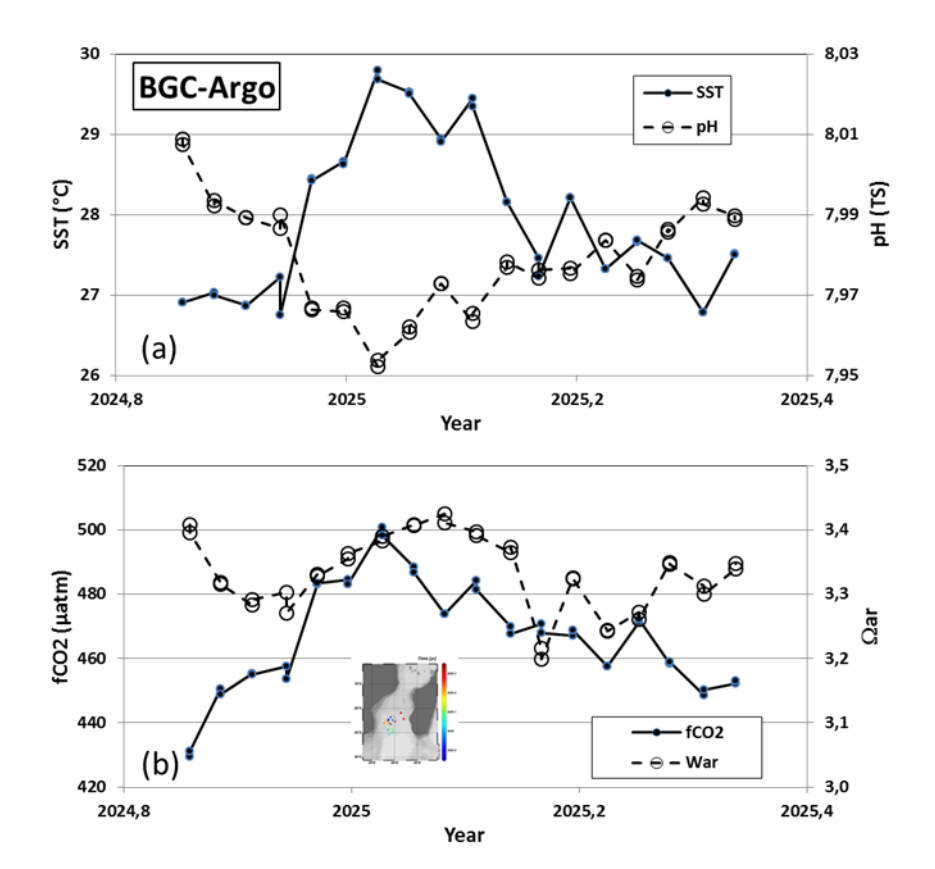
As of January 2025, the atmospheric  $CO_2$  is 426 ppm and 450 ppm should be reached in 2030 in the high scenario SSP5-8.5 (Figure 8a). In a global ocean model it has been suggested that at 450 ppm  $\Omega_{ar}$  would be around 3 in the South Indian Ocean and the Mozambique Channel, against 4 for pre-industrial  $\Omega_{ar}$  (Figure 4 in Hoegh-Guldberg et al., 2007). In our simulation, at 450 ppm,  $\Omega_{ar}$  is equal to 3.13 against 3.8 based on observations in May 1963. Extrapolating our result back in time, we estimated pH<sub>T</sub> at 8.18 and  $\Omega_{ar}$  equal to 4 at 280 ppm, close to the pre-industrial value estimated from dedicated reconstructions (Lo Monaco et al, 2021) or in global ocean models (Hoegh-Guldberg et al. 2007; Jiang et al, 2023).

Our calculation suggests that for a high emission scenario a risky level for corals ( $\Omega_{\rm ar}$  < 3, Hoegh-Guldberg et al., 2007) could be reached as soon as year 2034, i.e. in the next 10 years. This calls for maintaining regular carbonate system observations in this region, if possible at all seasons, in order to follow at best their evolution and the potential impact on the channel ecosystem and especially coral reefs in the context of global warming and acidification that will dramatically persist in the near future.

## 3.5 A large anomaly observed in 2025

As mentioned above, fCO<sub>2</sub> data are relatively sparse in the Mozambique Channel and should be obtained for all seasons. To complete the shipboard observations, biogeochemical (BGC) Argo floats have been developed and successfully used for 10 years for air-sea CO<sub>2</sub> flux estimates and/or acidification especially in the Southern Ocean in the frame of the SOCCOM project (e.g. Sarmiento et al, 2023; Mazloff et al, 2023; Metzl et al, 2025d). The floats record profiles down to 1000 or 2000 m at a 10-day frequency. In November 2024, a BGC-Argo float (WMO ID 7902123) was launched in the Mozambique Channel at 38.51°E/22.65°S (last profile used here recorded on 4th May 2025). The  $fCO_2$  and  $\Omega$ ar from the  $pH_T$  float data were calculated using CO2sys as for the shipboard data (section 2.3). Interestingly, the float recorded high temperature in January 2025 (up to 29.8°C, Figure 9a), a signal probably linked to a MHW (Figure S10) that occurred at high frequency in this region (Mawren et al, 2022). Sea surface temperature from reanalysis products suggests a temperature as high as 31°C in this region in January 2025 (Figure S10). Consequently, the sea surface fCO<sub>2</sub> derived from the float pH<sub>T</sub> data reached values above 480 μatm (Figure 9b). This leads to a strong CO₂ source anomaly, in line with CO<sub>2</sub> fluxes anomalies associated to MHW in the South Indian subtropics (e.g. Li et al, 2024). The lowest pH<sub>T</sub> of 7.95 was recorded on 11<sup>th</sup> January 2025, i.e. lower than the pH<sub>T</sub> derived from the FFNN model (Figure 7b). The aragonite saturation state derived from the BGC-Argo data reached 3.2 in March 2025, the same as that which we estimate in 2025 from the simulation (Figure 8d). The observations from the BGC-Argo offer important information to complement the shipboard data and should be used along with SOCAT data to test constraint data-based products.

Figure 9: Time-series of (a) SST and  $pH_T$ , and (b)  $fCO_2$  and  $\Omega_{ar}$  in the southern Mozambique Channel based on BGC-Argo data (WMO7902123) in November 2024 to May 2025 (location of data in the insert map). Data from https://www.mbari.org/products/data-repository/, last access 9/5/2025.



## 4. Summary and concluding remarks

New observations in 2021 and 2022 and historical  $fCO_2$  data available since 1963 in the Mozambique Channel were used to evaluate the decadal trends of the carbonate system in this region. With adapted  $A_T/S$  relationship for this region, we calculated  $C_T$  concentrations,  $pH_T$  and  $\Omega_{ar}$ . This calculation is first validated with in-situ  $A_T$  and  $C_T$  measurements obtained in January 2004, April 2019 and January 2021. Based on the data in January 2004 and 2021, we found a  $pH_T$  decrease of 0.032 (using  $fCO_2$  data) and -0.040 (using  $A_T$   $C_T$  data) over 17 years. Because the seasonality is large, the decadal trends based on  $fCO_2$  observations in 1963-2022 are evaluated for one season only (April-May). A FFNN model that reconstructed the monthly fields of the carbonate system is also used to investigate the trends for all seasons, but restricted to the period 1985-2023.

In this region where the ocean is a permanent  $CO_2$  sink of -0.25 (±0.06) molC.m<sup>-2</sup>.yr<sup>-1</sup>, fCO<sub>2</sub> observations available in April-May translate an acceleration of the acidification ranging from -0.012 decade<sup>-1</sup> in 1963-1995 to -0.027 (±0.003) decade<sup>-1</sup> in 1995-2022. Result from the FFNN model for all seasons suggest smaller pH<sub>T</sub> trends but, like in the observations, the decrease of pH<sub>T</sub> was faster in recent decades, -0.011 decade<sup>-1</sup> over 1985-1995 and -0.018 decade<sup>-1</sup> over 1995-2022. The FFNN model also suggests a faster trend in austral winter when the ocean  $CO_2$  sink is stronger and when the aragonite saturation state ( $\Omega_{ar}$ ) is low. In May 2022 we estimated  $\Omega_{ar}$  = 3.49, about 0.3 lower than observed in May 1963 ( $\Omega_{ar}$  = 3.86). The lowest  $\Omega_{ar}$  value of 3.23 was evaluated from the FFNN model in September 2023 that corresponds to the potential critical threshold value (3.25) for net reef accretion (Hoegh-Gulberg et al 2007) and could conduct to net reef dissolution (Eyre et al. 2018; Tribollet et al. 2019; Cornwall et al 2021).

A simple reconstruction and projection of the  $C_T$  concentrations based on anthropogenic  $CO_2$  in subsurface water and emissions scenario, suggests that the aragonite saturation state could be as low as 3 in the next 10 years. Following a previous work (Lo Monaco et al, 2021), the new data

presented here clearly reveal the progressive acidification in the Mozambique Channel and its acceleration in the recent decade with potential impacts on ecosystem including corals reefs areas like at Europa and Bassa de India. In a context where there is no sign of a slowdown in anthropogenic emissions, this already obvious acidification is alarming for the ocean health (Gattuso et al, 2015) and potential feedback on the ocean carbon cycle in general (e.g. Barrett et al, 2025). Understanding and quantifying the future response of phytoplanktonic and reef species in the context of global warming and acidification calls for adapted ocean biogeochemical models (Cornwall et al 2021) to take into account dynamics of bioerosion processes (see Schönberg et al 2017). In the Mozambique Channel, observations are still very sparse and the new observations presented here, including recent BGC-Agro data, offer important information to validate regional and global biogeochemical models that are not yet able to simulate correctly the seasonal cycle and decadal variability of the oceanic carbonate system. We strongly claim for maintaining regular sampling of ocean carbonate system parameters to reduce the model uncertainties and for adapted strategies at both scientific and political actions in the future.

#### Data availability:

748

749

750

751

752

753

754

755

756

757

758

759

760

761

762763

764

765

766

767 768

769

770

771

772

773

774

775776

777

778

779

780

781 782

783 784

785

786

787

788

789

790

791

792

793

794

795

796

797

Data used in this study are available in SOCAT (Bakker et al, 2016, www.socat.info) for fCO<sub>2</sub> surface data, in GLODAP (Lauvset et al, 2022a, 2022b, www.glodap.info) for water-column data. The  $A_T$  and C<sub>T</sub> underway data from OISO and CLIM-EPARSES cruises are available in Seanoe (Metzl et al. 2025c, https://www.seanoe.org, https://doi.org/10.17882/95414 and https://doi.org/10.17882/102337). The BGC-Argo float data with derived carbon parameters are available from SOCCOM (https://soccom.org, https://www.mbari.org/products/data-repository/). The CMEMS-LSCE-FFNN are available at E.U. Copernicus Marine Service (https://resources.marine.copernicus.eu/products, https://doi.org/10.48670/moi-00047). The Mixed layer depth data publicly available on **CMEMS** are the website: https://data.marine.copernicus.eu/product/ (Multi Observation Global Ocean ARMOR3D L4 MULTIOBS\_GLO\_PHY\_TSUV\_3D\_MYNRT\_015\_012).

### **Authors contributions:**

CLM and NM are co-investigators of the ongoing OISO project. AT was chief scientist of the CLIM-EPARSES 2019 cruise and JFT was chief scientist of the RESILIENCE cruise. MG and FC developed the CMEMS-LSCE-FFNN model and provided the model results. NM started the analysis, wrote the draft of the manuscript and prepared the figures with contributions from all co-authors.

**Competing interest:** The authors declare that they have no conflict of interest.

Acknowledgments: The OISO program was supported by the French institutes INSU (Institut National des Sciences de l'Univers) and IPEV (Institut Polaire Paul-Emile Victor), OSU Ecce-Terra (at Sorbonne Université), the French programs SOERE/Great-Gases and ICOS-France. We thank the French Oceanographic for financial and logistic support the OISO program (https://campagnes.flotteoceanographique.fr/series/228/). **CLIM-EPARSES** The supported by TAAF (Terres Australes et Antarctic Françaises), IRD (Institut de Recherche pour le Développement), Fondation Prince Albert II de Monaco (www.fpa2.org), INSU (Institut National des Sciences de l'Univers), CNRS (Centre National de Recherche Scientifique), Museum National d'Histoire Naturelle (MNHN), UMRs LOCEAN-IPSL, ENTROPIE and LSCE. The RESILIENCE cruise (https://doi.org/10.17600/18001917) was supported by the French National Oceanographic Fleet, by the Belmont Forum Ocean Front Change project, by the ISblue project and by the French National program LEFE (Les Enveloppes Fluides et l'Environnement). We thank the captains and crew of R.R.V. Marion-Dufresne and the staff at IFREMER, GENAVIR and IPEV. We also thank Guillaume Barut, Jonathan Fin and Claude Mignon for their help during the OISO, CLIM-EPARSES and RESILIENCE cruises. The development of the neural network model benefited from funding by the French INSU-GMMC project "PPR-Green-Grog (grant no 5-DS-PPR-GGREOG), the EU H2020 project AtlantOS (grant no 633211), as well as through the Copernicus Marine Environment Monitoring Service (project 83-CMEMS-TAC-MOB). We acknowledge the Southern Ocean Carbon and Climate Observations and Modeling (SOCCOM) Project funded by the National Science Foundation, Division of Polar Programs (NSF PLR-1425989 and OPP-1936222). We thank all colleagues who contributed to the quality control of ocean data made available through GLODAP (www.glodap.info). The Surface Ocean CO<sub>2</sub> Atlas (SOCAT, www.socat.info) is an international effort, endorsed by the International Ocean Carbon Coordination Project (IOCCP), the Surface Ocean Lower Atmosphere Study (SOLAS) to deliver a uniformly quality-controlled surface ocean CO2 database. We thank Hermann Bange associate editor, and anonymous reviewers for their positive reports and comments that helped revising the manuscript.

#### References

Alaguarda, D., Brajard, J., Coulibaly, G., Canesi, M., Douville, E., Le Cornec, F., Lelabousse, C. and Tribollet, A.:54 years of microboring community history explored by machine learning in a massive coral from Mayotte (Indian Ocean). Front. Mar. Sci. 9:899398. doi: 10.3389/fmars.2022.899398, 2022

Bakker, D. C. E., B. Pfeil, K. Smith, S. Hankin, A. Olsen, S. R. Alin, C. Cosca, B. Hales, S. Harasawa, A. Kozyr, Y. Nojiri, K. M. O'Brien, U. Schuster, M. Telszewski, B. Tilbrook, C. Wada, J. Akl, L. Barbero, N. Bates, J. Boutin, W.-J. Cai, R. D. Castle, F. P. Chavez, L. Chen, M. Chierici, K. Currie, H. J. W. De Baar, W. Evans, R. A. Feely, A. Fransson, Z. Gao, N. Hardman-Mountford, M. Hoppema, W.-J. Huang, C. W. Hunt, B. Huss, T. Ichikawa, A. Jacobson, T. Johannessen, E. M. Jones, S. Jones, Sara Jutterstrøm, V. Kitidis, A. Körtzinger, S. K. Lauvset, N. Lefèvre, A. B. Manke, J. T. Mathis, L. Merlivat, N. Metzl, P. Monteiro, A. Murata, T. Newberger, T. Ono, G.-H. Park, K. Paterson, D. Pierrot, A. F. Ríos, C.L. Sabine, S. Saito, J. Salisbury, V. V. S. S. Sarma, R. Schlitzer, R. Sieger, I. Skjelvan, T. Steinhoff, K. Sullivan, S. C. Sutherland, T. Suzuki, A. J. Sutton, C. Sweeney, T. Takahashi, J. Tjiputra, N. Tsurushima, S. M. A. C. van Heuven, D. Vandemark, P. Vlahos, D. W. R. Wallace, R. Wanninkhof and A. J. Watson: An update to the Surface Ocean CO2 Atlas (SOCAT version 2). Earth System Science Data, 6, 69-90. doi:10.5194/essd-6-69-2014. 2014

Bakker, D. C. E., Pfeil, B., Landa, C. S., Metzl, N., O'Brien, K. M., Olsen, A., Smith, K., Cosca, C., Harasawa, S., Jones, S. D., Nakaoka, S.-I., Nojiri, Y., Schuster, U., Steinhoff, T., Sweeney, C., Takahashi, T., Tilbrook, B., Wada, C., Wanninkhof, R., Alin, S. R., Balestrini, C. F., Barbero, L., Bates, N. R., Bianchi, A. A., Bonou, F., Boutin, J., Bozec, Y., Burger, E. F., Cai, W.-J., Castle, R. D., Chen, L., Chierici, M., Currie, K., Evans, W., Featherstone, C., Feely, R. A., Fransson, A., Goyet, C., Greenwood, N., Gregor, L., Hankin, S., Hardman-Mountford, N. J., Harlay, J., Hauck, J., Hoppema, M., Humphreys, M. P., Hunt, C. W., Huss, B., Ibánhez, J. S. P., Johannessen, T., Keeling, R., Kitidis, V., Körtzinger, A., Kozyr, A., Krasakopoulou, E., Kuwata, A., Landschützer, P., Lauvset, S. K., Lefèvre, N., Lo Monaco, C., Manke, A., Mathis, J. T., Merlivat, L., Millero, F. J., Monteiro, P. M. S., Munro, D. R., Murata, A., Newberger, T., Omar, A. M., Ono, T., Paterson, K., Pearce, D., Pierrot, D., Robbins, L. L., Saito, S., Salisbury, J., Schlitzer, R., Schneider, B., Schweitzer, R., Sieger, R., Skjelvan, I., Sullivan, K. F., Sutherland, S. C., Sutton, A. J., Tadokoro, K., Telszewski, M., Tuma, M., Van Heuven, S. M. A. C., Vandemark, D., Ward, B., Watson, A. J., Xu, S., 2016. A multi-decade record of high-quality fCO<sub>2</sub> data in version 3 of the Surface Ocean CO<sub>2</sub> Atlas (SOCAT), Earth Syst. Sci. Data, 8, 383-413, doi:10.5194/essd-8-383-2016.

Bakker, Dorothee C. E.; Alin, Simone R.; Bates, Nicholas; Becker, Meike; Gkritzalis, Thanos; Jones, Steve D.; Kozyr, Alex; Lauvset, Siv K.; Metzl, Nicolas; Nakaoka, Shin-ichiro; O'Brien, Kevin M.; Olsen, Are; Pierrot, Denis; Steinhoff, Tobias; Sutton, Adrienne J.; Takao, Shintaro; Tilbrook, Bronte; Wada, Chisato; Wanninkhof, Rik; Akl, John; Arbilla, Lisandro A.; Arruda, Ricardo; Azetsu-Scott, Kumiko; Barbero, Leticia; Beatty, Cory M.; Berghoff, Carla F.; Bittig, Henry C.; Burger, Eugene F.; Campbell,

- 850 Katie; Cardin, Vanessa; Collins, Andrew; Coppola, Laurent; Cronin, Margot; Cross, Jessica N.; Currie, 851 Kim I.; Emerson, Steven R.; Enright, Matt P.; Enyo, Kazutaka; Evans, Wiley; Feely, Richard A.; Flohr, 852 Anita; Gehrung, Martina; Glockzin, Michael; González-Dávila, Melchor; Hamnca, Siyabulela; Hartman, 853 Sue; Howden, Stephan D.; Kam, Kitty; Kamb, Linus; Körtzinger, Arne; Kosugi, Naohiro; Lefèvre, 854 Nathalie; Lo Monaco, Claire; Macovei, Vlad A.; Maenner Jones, Stacy; Manalang, Dana; Martz, Todd 855 R.; Mdokwana, Baxolele; Monacci, Natalie M.; Monteiro, Pedro M. S.; Mordy, Calvin; Morell, Julio M.; 856 Murata, Akihiko; Neill, Craig; Noh, Jae-Hoon; Nojiri, Yukihiro; Ohman, Mark; Olivier, Léa; Ono, 857 Tsuneo; Petersen, Wilhelm; Plueddemann, Albert J.; Prytherch, John; Rehder, Gregor; Rutgersson, 858 Anna; Santana-Casiano, J. Magdalena; Schlitzer, Reiner; Send, Uwe; Skjelvan, Ingunn; Sullivan, Kevin F.; T'Jampens, Michiel; Tadokoro, Kazuaki; Telszewski, Maciej; Theetaert, Hannelore; Tsanwani, 859 860 Mutshutshu; Vandemark, Douglas; van Ooijen, Erik; Veccia, Martín H.; Voynova, Yoana G.; Wang, 861 Hongjie; Weller, Robert A.; Woosley, Ryan J. 2024. Surface Ocean CO2 Atlas Database Version 2024 (SOCATv2024) (NCEI Accession 0293257). [indicate subset used]. NOAA National Centers for 862 863 Environmental Information. Dataset. https://doi.org/10.25921/9wpn-th28. Last Access 30 June 2024.
- Barrett, R. C., Carter, B. R., Fassbender, A. J., Tilbrook, B., Woosley, R. J., Azetsu-Scott, K., et al. (2025). Biological responses to ocean acidification are changing the global ocean carbon cycle. Global Biogeochemical Cycles, 39, e2024GB008358. https://doi.org/10.1029/2024GB008358

868

872

876

881

885

888

895

- Bates, N.R., Pequignet, A.C., and Sabine, C.L.: Ocean carbon cycling in the Indian Ocean: 1.
  Spatiotemporal variability of inorganic carbon and air-sea CO2 gas exchange. Global Biogeochem.
  Cycles 20, GB3020. <a href="https://doi.org/10.1029/2005GB002491">https://doi.org/10.1029/2005GB002491</a>, 2006
- Camp E.F., Schoepf, V., Mumby, P. J., Hardtke, L. A., Rodolfo-Metalpa, R., Smith, D. J. and Suggett, D. J.: The Future of Coral Reefs Subject to Rapid Climate Change: Lessons from Natural Extreme Environments. Front. Mar. Sci. 5:4. doi: 10.3389/fmars.2018.00004, 2018.
- Chakraborty, K., Joshi, A. P., Ghoshaln P. K., Baduru, B., Valsala, V., Sarma V. V. S. S., Metzl, N., Gehlen, M., Chevallier, F., Lo Monaco, C. Indian Ocean acidification and its driving mechanisms over the last four decades (1980-2019), Global Biogeochemical Cycles, 38, e2024GB008139. https://doi.org/10.1029/2024GB008139, 2024.
- Chau, T.-T.-T., Gehlen, M., Metzl, N., and Chevallier, F.: CMEMS-LSCE: a global, 0.25°, monthly reconstruction of the surface ocean carbonate system, Earth Syst. Sci. Data, 16, 121–160, https://doi.org/10.5194/essd-16-121-2024, 2024.
- Cheng, L., Abraham, J., Trenberth, K.E. et al. Record High Temperatures in the Ocean in 2024. Adv.
   Atmos. Sci. 42, 1092–1109. <a href="https://doi.org/10.1007/s00376-025-4541-3">https://doi.org/10.1007/s00376-025-4541-3</a>, 2025
- Copin-Montégut, C., 1988. A new formula for the effect of temperature on the partial pressure of CO2 in seawater. Marine Chemistry, 25, 29-37. https://doi.org/10.1016/0304-4203(88)90012-6.
- Copin-Montégut, C., 1989. A new formula for the effect of temperature on the partial pressure of CO2 in seawater. Corrigendum. Marine Chemistry, 27, 143-144. https://doi.org/10.1016/0304-4203(89)90034-0.
- Cornwall, C.E., S. Comeau, N.A. Kornder, C.T. Perry, R. van Hooidonk, T.M. DeCarlo, M.S. Pratchett, K.D. Anderson, N. Browne, R. Carpenter, G. Diaz-Pulido, J.P. D'Olivo, S.S. Doo, J. Figueiredo, S.A.V. Fortunato, E. Kennedy, C.A. Lantz, M.T. McCulloch, M. González-Rivero, V. Schoepf, S.G. Smithers, & R.J. Lowe, Global declines in coral reef calcium carbonate production under ocean acidification and warming, Proc. Natl. Acad. Sci. U.S.A. 118 (21) e2015265118, doi:10.1073/pnas.2015265118, 2021.

- Dickson, A. G., 1990. Standard potential of the reaction:  $AgCl(s) + \frac{1}{2}H2(g) = Ag(s) + HCl(aq)$ , and the standard acidity constant of the ion HSO4– in synthetic sea water from 273.15 to 318.15 K. J. Chem.
- 904 Thermodyn. 22: 113–127. doi:10.1016/0021-9614(90)90074-Z.

https://doi.org/10.5194/essd-2025-250, in review, 2025.

905

Doney, S.C., Busch, D.S., Cooley, S.R., Kroeker, K.J., 2020. The impacts of ocean acidification on marine ecosystems and reliant human communities. Annu. Rev. Environ. Resour. 45 (1). https://doi.org/10.1146/annurev-environ-012320-083019.

909

Doney, S.C., Fabry, V.J., Feely, R.A., Kleypas, J.A., 2009. Ocean acidification: The other CO2 problem.
Annu. Rev. Mar. Sci. 1 (1), 169–192. https://doi.org/10.1146/annurev.marine.010908.163834.

912

Edmond, J.M., 1970. High precision determination of titration alkalinity and total carbon dioxide content of sea water by potentiometric titration. Deep-Sea Res. 17, 737–750. https://doi.org/10.1016/0011-7471(70)90038-0.

916

Eyre, B.D., Cyronak, T., Drupp, P., De Carlo, E.H., Sachs, J.P., Andersson, A.J.: Coral reefs will transition one to net dissolving before end of century. Science 359 (6378), 908–911. https://doi.org/10.1126/science.aao1118. 2018

920

Fabry, V.J., Seibel, B.A., Feely, R.A., Orr, J.C., 2008. Impacts of ocean acidification on marine fauna and ecosystem processes. ICES J. Mar. Sci. 65, 414–432. https://doi.org/10.1093/icesjms/fsn048.

923

Fay, A. R., Munro, D. R., McKinley, G. A., Pierrot, D., Sutherland, S. C., Sweeney, C., and Wanninkhof,
 R.: Updated climatological mean ΔfCO2 and net sea—air CO2 flux over the global open ocean regions,
 Earth Syst. Sci. Data, 16, 2123–2139, https://doi.org/10.5194/essd-16-2123-2024, 2024.

927

Findlay, H.S., Feely, R.A., Jiang, L.-Q., Pelletier, G. and Bednaršek, N.: Ocean Acidification: Another Planetary Boundary Crossed. Glob Change Biol, 31: e70238. Doi: 10.1111/gcb.70238, 2025

930

931 Forster, P. M., Smith, C., Walsh, T., Lamb, W. F., Lamboll, R., Cassou, C., Hauser, M., Hausfather, Z., 932 Lee, J.-Y., Palmer, M. D., von Schuckmann, K., Slangen, A. B. A., Szopa, S., Trewin, B., Yun, J., Gillett, N. 933 P., Jenkins, S., Matthews, H. D., Raghavan, K., Ribes, A., Rogelj, J., Rosen, D., Zhang, X., Allen, M., 934 Aleluia Reis, L., Andrew, R. M., Betts, R. A., Borger, A., Broersma, J. A., Burgess, S. N., Cheng, L., 935 Friedlingstein, P., Domingues, C. M., Gambarini, M., Gasser, T., Gütschow, J., Ishii, M., Kadow, C., 936 Kennedy, J., Killick, R. E., Krummel, P. B., Liné, A., Monselesan, D. P., Morice, C., Mühle, J., Naik, V., 937 Peters, G. P., Pirani, A., Pongratz, J., Minx, J. C., Rigby, M., Rohde, R., Savita, A., Seneviratne, S. I., 938 Thorne, P., Wells, C., Western, L. M., van der Werf, G. R., Wijffels, S. E., Masson-Delmotte, V., and 939 Zhai, P.: Indicators of Global Climate Change 2024: annual update of key indicators of the state of the 940 climate system and human influence, Earth Syst. Sci. Data Discuss. [preprint],

941 942

955

943 Friedlingstein, P., O'Sullivan, M., Jones, M. W., Andrew, R. M., Hauck, J., Landschützer, P., Le Quéré, 944 C., Li, H., Luijkx, I. T., Olsen, A., Peters, G. P., Peters, W., Pongratz, J., Schwingshackl, C., Sitch, S., 945 Canadell, J. G., Ciais, P., Jackson, R. B., Alin, S. R., Arneth, A., Arora, V., Bates, N. R., Becker, M., 946 Bellouin, N., Berghoff, C. F., Bittig, H. C., Bopp, L., Cadule, P., Campbell, K., Chamberlain, M. A., 947 Chandra, N., Chevallier, F., Chini, L. P., Colligan, T., Decayeux, J., Djeutchouang, L. M., Dou, X., Duran 948 Rojas, C., Enyo, K., Evans, W., Fay, A. R., Feely, R. A., Ford, D. J., Foster, A., Gasser, T., Gehlen, M., 949 Gkritzalis, T., Grassi, G., Gregor, L., Gruber, N., Gürses, Ö., Harris, I., Hefner, M., Heinke, J., Hurtt, G. 950 C., Iida, Y., Ilyina, T., Jacobson, A. R., Jain, A. K., Jarníková, T., Jersild, A., Jiang, F., Jin, Z., Kato, E., 951 Keeling, R. F., Klein Goldewijk, K., Knauer, J., Korsbakken, J. I., Lan, X., Lauvset, S. K., Lefèvre, N., Liu, 952 Z., Liu, J., Ma, L., Maksyutov, S., Marland, G., Mayot, N., McGuire, P. C., Metzl, N., Monacci, N. M., 953 Morgan, E. J., Nakaoka, S.-I., Neill, C., Niwa, Y., Nützel, T., Olivier, L., Ono, T., Palmer, P. I., Pierrot, D., Qin, Z., Resplandy, L., Roobaert, A., Rosan, T. M., Rödenbeck, C., Schwinger, J., Smallman, T. L., Smith, 954

956 Tian, H., Tilbrook, B., Torres, O., Tourigny, E., Tsujino, H., Tubiello, F., van der Werf, G., Wanninkhof, 957 R., Wang, X., Yang, D., Yang, X., Yu, Z., Yuan, W., Yue, X., Zaehle, S., Zeng, N., and Zeng, J.: Global 958 Carbon Budget 2024, Earth Syst. Sci. Data, 17, 965-1039, https://doi.org/10.5194/essd-17-965-2025,

959 2025.

960

961 Gattuso, J.-P., Magnan, A., Billé, R., Cheung, W. W. L., Howes, E. L., Joos, F., Allemand, D., Bopp, L., 962 Cooley, S., Eakin, M., Hoegh-Guldberg, O., Kelly, R. P., Pörtner, H.-O., Rogers, A. D., Baxter, J. M., Laffoley, D., Osborn, D., Rankovic, A., Rochette, J., Sumaila, U. R., Treyer, S., and Turley, C.: 963 964 Contrasting futures for ocean and society from different anthropogenic CO2 emissions scenarios, 965 Science, 349, aac4722, https://doi.org/10.1126/science.aac4722, 2015.

966 967 Hoegh-Guldberg, O., P. J. Mumby, A. J. Hooten, R. S. Steneck, P. Greenfield, E. Gomez, C. D. Harvell, 968 P. F. Sale, A. J. Edwards, K. Caldeira, N. Knowlton, C. M. Eakin, R. Iglesias-Prieto, N. Muthiga, R. H.

969 Bradbury, A. Dubi and M. E. Hatziolos: Coral Reefs Under Rapid Climate Change and Ocean 970

Acidification. Science, 14, 1737-1742, doi:10.1126/science.1152509, 2007

971

972 lida, Y., Takatani, Y., Kojima, A., and Ishii, M.: Global trends of ocean CO2 sink and ocean acidification: 973 an observation based reconstruction of surface ocean inorganic carbon variables, J. Oceanogr., 77, 974 323-358, https://doi.org/10.1007/s10872-020-00571-5, 2021.

975

976 Jiang, L.-Q., Dunne, J., Carter, B. R., Tjiputra, J. F., Terhaar, J., Sharp, J. D., et al., 2023. Global surface ocean acidification indicators from 1750 to 2100. Journal of Advances in Modeling Earth Systems, 15, 977 978 e2022MS003563. https://doi.org/10.1029/2022MS003563.

979

Keeling, C. D., Waterman, L. S., 1968. Carbon dioxide in surface ocean waters: 3. Measurements on 980 Lusiad Expedition 1962–1963, J. Geophys. Res., 73(14), 4529–4541, doi:10.1029/JB073i014p04529. 981

982

983 Kwiatkowski, L., Torres, O., Bopp, L., Aumont, O., Chamberlain, M., Christian, J. R., Dunne, J. P., 984 Gehlen, M., Ilyina, T., John, J. G., Lenton, A., Li, H., Lovenduski, N. S., Orr, J. C., Palmieri, J., Santana-985 Falcón, Y., Schwinger, J., Séférian, R., Stock, C. A., Tagliabue, A., Takano, Y., Tjiputra, J., Toyama, K., 986 Tsujino, H., Watanabe, M., Yamamoto, A., Yool, A., and Ziehn, T.: Twenty-first century ocean 987 warming, acidification, deoxygenation, and upper-ocean nutrient and primary production decline 988 from CMIP6 model projections, Biogeosciences, 17, 3439-3470, https://doi.org/10.5194/bg-17-3439-989 2020, 2020.

990

991 Lan, X., Tans, P. and K.W. Thoning: Trends in globally-averaged CO2 determined from NOAA Global 992 05-May-2025 Monitoring Laboratory measurements. Version Monday, 16:38:58 MDT 993 https://doi.org/10.15138/9N0H-ZH07, 2025

994

995 Lauvset, S. K., Gruber, N., Landschützer, P., Olsen, A., and Tjiputra, J.: Trends and drivers in global 996 surface ocean pH over the past 3 decades. Biogeosciences, 12, 1285-1298, doi:10.5194/bg-12-1285-997 2015, 2015

998

999 Lauvset, S. K., Lange, N., Tanhua, T., Bittig, H. C., Olsen, A., Kozyr, A., Alin, S., Álvarez, M., Azetsu-1000 Scott, K., Barbero, L., Becker, S., Brown, P. J., Carter, B. R., da Cunha, L. C., Feely, R. A., Hoppema, M., 1001 Humphreys, M. P., Ishii, M., Jeansson, E., Jiang, L.-Q., Jones, S. D., Lo Monaco, C., Murata, A., Müller, 1002 J. D., Pérez, F. F., Pfeil, B., Schirnick, C., Steinfeldt, R., Suzuki, T., Tilbrook, B., Ulfsbo, A., Velo, A., 1003 Woosley, R. J., and Key, R. M.: GLODAPv2.2022: the latest version of the global interior ocean 1004 biogeochemical data product, Earth Syst. Sci. Data, 14, 5543-5572, https://doi.org/10.5194/essd-14-1005 5543-2022, 2022a.

- Lauvset, Siv K.; Lange, Nico; Tanhua, Toste; Bittig, Henry C.; Olsen, Are; Kozyr, Alex; Alin, Simone R.;
- 1008 Álvarez, Marta; Azetsu-Scott, Kumiko; Barbero, Leticia; Becker, Susan; Brown, Peter J.; Carter,
- Brendan R.; Cotrim da Cunha, Leticia; Feely, Richard A.; Hoppema, Mario; Humphreys, Matthew P.;
- 1010 Ishii, Masao; Jeansson, Emil; Jiang, Li-Qing; Jones, Steve D.; Lo Monaco, Claire; Murata, Akihiko;
- Müller, Jens Daniel; Pérez, Fiz F.; Pfeil, Benjamin; Schirnick, Carsten; Steinfeldt, Reiner; Suzuki, Toru;
- Tilbrook, Bronte; Ulfsbo, Adam; Velo, Antón; Woosley, Ryan J.; Key, Robert M. (2022). Global Ocean
- Data Analysis Project version 2.2022 (GLODAPv2.2022) (NCEI Accession 0257247). [indicate subset
- 1014 used]. NOAA National Centers for Environmental Information. [Dataset].
- 1015 https://doi.org/10.25921/1f4w-0t92. Last Access [4 June 2025], 2022b
- 1016
- 1017 Li, C., Burger, F. A., Raible, C. C., and Frölicher, T. L.: Observed regional impacts of marine heatwaves
- 1018 on sea-air CO2 exchange. Geophysical Research Letters, 51, e2024GL110379.
- 1019 https://doi.org/10.1029/2024GL110379, 2024
- 1020
- Lo Monaco, C., Metzl, N., Fin, J., Mignon, C., Cuet, P., Douville, E., Gehlen, M., Trang Chau, T.T.,
- 1022 Tribollet, A., 2021. Distribution and long-term change of the sea surface carbonate system in the
- 1023 Mozambique Channel (1963-2019), Deep-Sea Research Part II,
- 1024 https://doi.org/10.1016/j.dsr2.2021.104936.

- 1026 Lueker, T.J., Dickson, A.G., Keeling, C.D., 2000. Ocean pCO(2) calculated from dissolved inorganic
- 1027 carbon, alkalinity, and equations for K-1 and K-2: validation based on laboratory measurements of
- 1028 CO2 in gas and seawater at equilibrium. Marine Chemistry 70, 105-119.
- 1029 https://doi.org/10.1016/S0304-4203(00)00022-0.

1030

- 1031 Ma, D., Gregor, L., and Gruber, N.: Four decades of trends and drivers of global surface ocean
- acidification. Global Biogeochemical Cycles, 37, e2023GB007765. 10.1029/2023GB007765, 2023

1033

- Mawren, D., Hermes, J. & Reason, C.J.C. Marine heatwaves in the Mozambique Channel. Clim Dyn
- 1035 (2022). https://doi.org/10.1007/s00382-021-05909-3

1036

- 1037 Mazloff, M. R., Verdy, A., Gille, S. T., Johnson, K. S., Cornuelle, B. D., and Sarmiento, J.: Southern
- 1038 Ocean acidification revealed by biogeochemical-Argo floats. Journal of Geophysical Research:
- 1039 Oceans, 128, e2022JC019530. https://doi.org/10.1029/2022JC019530, 2023.

1040

- 1041 Meinshausen, M., Nicholls, Z. R. J., Lewis, J., Gidden, M. J., Vogel, E., Freund, M., et al.: The shared
- 1042 socioeconomic pathway (SSP) greenhouse gas concentrations and their extensions to 2500.
- 1043 Geoscientific Model Development, 13(8), 3571–3605. https://doi.org/10.5194/gmd-13-3571-2020,
- 1044 2020.

1045

- 1046 Metzl, N., Louanchi, F., and Poisson, A.: Seasonal and interannual variations of sea surface carbon
- dioxide in the subtropical indian ocean. Mar. Chem. 60, 131–146. https://doi.org/10.1016/S0304-
- 1048 4203(98)00083-8., 1998

1049

- 1050 Metzl, N.: Decadal increase of oceanic carbon dioxide in Southern Indian Ocean surface waters
- 1051 (1991–2007), Deep-Sea Res. Pt. II, 56, 607–619, https://doi.org/10.1016/j.dsr2.2008.12.007, 2009.

1052

- 1053 Metzl, N., Lo Monaco, C., Tribollet, A., and Kartavtseff A.. CLIM-EPARSES 1 cruise: S-ADCP data.
- 1054 SEANOE. <a href="https://doi.org/10.17882/89702">https://doi.org/10.17882/89702</a>, 2022

- Metzl, N., Fin, J., Lo Monaco, C., Mignon, C., Alliouane, S., Bombled, B., Boutin, J., Bozec, Y., Comeau,
- 1057 S., Conan, P., Coppola, L., Cuet, P., Ferreira, E., Gattuso, J.-P., Gazeau, F., Goyet, C., Grossteffan, E.,
- Lansard, B., Lefèvre, D., Lefèvre, N., Leseurre, C., Petton, S., Pujo-Pay, M., Rabouille, C., Reverdin, G.,
- Ridame, C., Rimmelin-Maury, P., Ternon, J.-F., Touratier, F., Tribollet, A., Wagener, T., and Wimart-
- 1060 Rousseau, C.: An updated synthesis of ocean total alkalinity and dissolved inorganic carbon

measurements from 1993 to 2023: the SNAPO-CO2-v2 dataset, Earth Syst. Sci. Data, 17, 1075–1100, https://doi.org/10.5194/essd-17-1075-2025, 2025a.

1063

1064 Metzl, N., C. Lo Monaco, G. Barut and J.-F. Ternon: Contrasting trends of the ocean CO2 sink and pH 1065 in the Agulhas current system and the Mozambique Basin, South-Western Indian Ocean (1963-2023). 1066 Deep Sea Research Part II: Topical **Studies** in Oceanography, 105459, 1067 https://doi.org/10.1016/j.dsr2.2025.105459, 2025b

1068

Metzl, N., Fin, J., Lo Monaco, C., Mignon, C., Alliouane, S., Bombled B., Boutin, J., Bozec, Y., Comeau, S., Conan, P., Coppola, L., Cuet, P., Ferreira, E., Gattuso, J.-P., Gazeau, F., Goyet, C., Grossteffan, E., Lansard, B., Lefèvre, D., Lefèvre, N., Leseurre, C., Lombard, F., Petton, S., Pujo-Pay, M., Rabouille, C., Reverdin, G., Ridame, C., Rimmelin-Maury, P., Ternon, J.-F., Touratier, F., Tribollet, A., Wagener, T., and Wimart-Rousseau, C.: An updated synthesis of ocean total alkalinity and dissolved inorganic carbon measurements from 1993 to 2023: the SNAPO-CO2-v2 dataset. SEANOE. [dataset], Last Access [4 June 2025], https://doi.org/10.17882/102337, 2025c.

1076

Metzl, N., C. Lo Monaco, C. Leseurre, G. Barut, G. Reverdin, C. Ridame, and L. Talley: Anthropogenic
 CO2 and acidification in the Southern Indian Ocean: combining ship-board and BGC-Argo float data,
 Glob. Biog. Cycl., in rev. 2025GB008606. 2025d

1080

Millero, F. J., Lee, K., Roche, M.: Distribution of alkalinity in the surface waters of the major oceans.

Mar. Chem. 60, 111–130. <a href="https://doi.org/10.1016/S0304-4203(97)00084-4">https://doi.org/10.1016/S0304-4203(97)00084-4</a>, 1998

1083

Murata, A., Kumamoto, Y., Sasaki, K., Watanabe, S., and Fukasawa, M.:Decadal increases in anthropogenic CO2 along 20°S in the SouthSouth Indian ocean. J. Geophys. Res. 115, C12055. https://doi.org/10.1029/2010JC006250, 2010

1087

1088 Pfeil, B., Olsen, A., Bakker, D. C. E., Hankin, S., Koyuk, H., Kozyr, A., Malczyk, J., Manke, A., Metzl, N., 1089 Sabine, C. L., Akl, J., Alin, S. R., Bates, N., Bellerby, R. G. J., Borges, A., Boutin, J., Brown, P. J., Cai, W.-1090 J., Chavez, F. P., Chen, A., Cosca, C., Fassbender, A. J., Feely, R. A., González-Dávila, M., Goyet, C., 1091 Hales, B., Hardman-Mountford, N., Heinze, C., Hood, M., Hoppema, M., Hunt, C. W., Hydes, D., Ishii, M., Johannessen, T., Jones, S. D., Key, R. M., Körtzinger, A., Landschützer, P., Lauvset, S. K., Lefèvre, 1092 1093 N., Lenton, A., Lourantou, A., Merlivat, L., Midorikawa, T., Mintrop, L., Miyazaki, C., Murata, A., 1094 Nakadate, A., Nakano, Y., Nakaoka, S., Nojiri, Y., Omar, A. M., Padin, X. A., Park, G.-H., Paterson, K., 1095 Perez, F. F., Pierrot, D., Poisson, A., Ríos, A. F., Santana-Casiano, J. M., Salisbury, J., Sarma, V. V. S. S., 1096 Schlitzer, R., Schneider, B., Schuster, U., Sieger, R., Skjelvan, I., Steinhoff, T., Suzuki, T., Takahashi, T., 1097 Tedesco, K., Telszewski, M., Thomas, H., Tilbrook, B., Tjiputra, J., Vandemark, D., Veness, T., 1098 Wanninkhof, R., Watson, A. J., Weiss, R., Wong, C. S., Yoshikawa-Inoue, H.: A uniform, quality 1099 controlled Surface Ocean CO2 Atlas (SOCAT), Earth Syst. Sci. Data, 5, 125-143, doi:10.5194/essd-5-1100 125-2013, 2013

1101

Orr, J. C., Epitalon, J.-M., Dickson, A. G., and Gattuso, J.-P.: Routine uncertainty propagation for the marine carbon dioxide system, Marine Chemistry, Vol. 207, 84-107, doi:10.1016/j.marchem.2018.10.006, 2018.

1105

Poisson, A., Metzl, N., Brunet, C., Schauer, B., Bres, B., Ruiz-Pino, D., and Louanchi, F.: Variability of sources and sinks of CO2 in the western Indian and southern oceans during the year 1991, J. Geophys. Res., 98(C12), 22759–22778, doi:10.1029/93JC02501, 1993

1109

Revelle, R., and Suess, H.E.: Carbon dioxide exchange between atmosphere and ocean and the question of an increase of atmospheric CO2 during the past decades. Tellus 9, 18–27. <a href="https://doi.org/10.1111/j.2153-3490.1957.tb01849.x">https://doi.org/10.1111/j.2153-3490.1957.tb01849.x</a>, 1957

- Sarmiento, J.L., Johnson, K.S., Arteaga, L.A., Bushinsky, S.M., Cullen, H.M., Gray, A.R., Hotinski, R.M.,
- Maurer, T.L., Mazloff, M.R., Riser, S.C., Russell, J.L., Schofield, O.M., Talley, L.D., The Southern Ocean
- 1116 Carbon and Climate Observations and Modeling (SOCCOM) project: A review, Progress in
- 1117 Oceanography, doi: https://doi.org/10.1016/j.pocean.2023.103130, 2023.

1119 Schlitzer, R., 2018. Ocean Data View, http://odv.awi.de.

1120

- Schönberg, C.H.L., Fang, J.K.H., Carreiro-Silva, M., Tribollet, A., Wisshak, M.: Bioerosion: the other ocean acidification problem. ICES (Int. Counc. Explor. Sea) J. Mar. Sci. fsw254
- 1123 https://doi.org/10.1093/icesjms/fsm254, 2017

1124

- Strahl, J., Stolz, I., Uthicke, S., Vogel, N., Noonan, S. H. C., Fabricius, K. E.: Physiological and ecological performance differs in four coral taxa at a volcanic carbon dioxide seep. COMPARATIVE
- 1127 BIOCHEMISTRY AND PHYSIOLOGY A-MOLECULAR & INTEGRATIVE PHYSIOLOGY, 184, 179-186,,
- 1128 10.1016/j.cbpa.2015.02.018, 2015

1129

- Takahashi, T., Olafsson, J., Goddard, J. G., Chipman, D. W., and Sutherland, S. C.: Seasonal variation of
- 1131 CO2 and nutrients in the high-latitude surface oceans: A comparative study, Global Biogeochem.
- 1132 Cycles, 7(4), 843–878, doi:10.1029/93GB02263, 1993

1133

- 1134 Takahashi, T., Sutherland, S. C., Sweeney, C., Poisson, A., Metzl, N., Tilbrook, B., Bates,
- 1135 N., Wanninkhof, R., Feely, R. A., Sabine, C., Olafsson, J., and Nojiri, Y.: Global Sea-Air CO2 Flux Based
- on Climatological Surface Ocean pCO2, and Seasonal Biological and Temperature Effect, Deep-Sea
- 1137 Res. Pt. II, 49, 9–10, 1601–1622, https://doi.org/10.1016/S0967-0645(02)00003-6, 2002.

1138

- 1139 Ternon, J.-F., Noyon, M., Penven, P., Herbette, S., Artigas, L. F., Toullec, J., et al.: Resilience fRonts,
- 1140 EddieS and marIne LIfe in the wEstern iNdian oCEan. In 19 April—24 May 2022, MD237 R/V marion
- 1141 Dufresne (Tech. Rep.). Cruise report, 107 pp., https://doi.org/10.17600/18001917, 2023

1142

- Tilbrook, B., E. B. Jewett , M. D. DeGrandpre, J. M. Hernandez-Ayon, , R. A. Feely, D. K. Gledhill, L.
- 1144 Hansson, K. Isensee, M. L. Kurz, J. A. Newton, S. A. Siedlecki, F. Chai, S. Dupont, M. Graco, E. Calvo, D.
- Greeley, L. Kapsenberg, M. Lebrec, C. Pelejero, K. L. Schoo, M. Telszewski:. An Enhanced Ocean
- 1146 Acidification Observing Network: From People to Technology to Data Synthesis and Information
- 1147 Exchange. Frontiers in Marine Science, 6, 337, DOI:10.3389/fmars.2019.00337, 2019

1148

- Touratier, F., Azouzi, L., Goyet, C.: CFC-11, Δ14C and 3H tracers as a means to assess anthropogenic
- 1150 CO2 concentrations in the ocean. Tellus B, 59(2), 318-325, doi:10.1111/j.1600-0889.2006.00247.x,
- 1151 2007.

1152

- 1153 Tribollet, A., C. Godinot, M. Atkinson, and C. Langdon: Effects of elevated pCO2 on dissolution of
- 1154 coral carbonates by microbial euendoliths, Global Biogeochem. Cycles, 23, GB3008,
- 1155 doi:10.1029/2008GB003286, 2009

1156

- 1157 Tribollet, A., Chauvin, A., Cuet, P.: Carbonate dissolution by reef microbial borers: a biogeological
- 1158 process producing alkalinity under different pCO2 conditions. Facies 65, 2.
- 1159 https://doi.org/10.1007/s10347-018-0548-x, 2019

1160

- 1161 Uppström, L. R., 1974. The boron/chlorinity ratio of deep-sea water from the Pacific Ocean, Deep Sea
- 1162 Research and Oceanographic Abstracts, 21, 161–162, https://doi.org/10.1016/0011-7471(74)90074-
- 1163 6.